Summer 8-22-2021

Patterns of torso morphology in extant quadrupedal amniotes and their paleontological applications

Myles M.A. Walsh
DePaul University, mwalsh50@mail.depaul.edu

Patterns of torso morphology in extant quadrupedal amniotes and their paleontological applications

A Thesis Presented in

Partial Fulfillment of the

Requirements for the Degree of

Master of Science

July 2021

By

Myles M.A. Walsh

Thesis Advisor: Kenshu Shimada, Ph.D.

Department of Biological Sciences

College of Science and Health

DePaul University

Chicago, Illinois

Table of Contents

List of Tables

List of Figures

List of Appendices

Acknowledgements

I received a tremendous amount of assistance and support throughout the duration of this research. A large portion of this study took place as we navigated a challenging time due to the COVID-19 pandemic, yet so many people rose to the occasion and were integral in helping me get to this point. I would first like to thank my professors from DePaul University's Department of Biological Sciences and the College of Science and Health for the financial support and for providing a foundational framework and challenging me to achieve academic success. Thank you to my committee members, Drs. Windsor Aguirre and Timothy Sparkes, for their feedback and help with developing this project. I would also like to thank my advisor, Dr. Kenshu Shimada, for his guidance and insights during every stage of this project and for allowing me to explore my own interests. Your generosity and willingness to accompany me on data collecting excursions was absolutely a highlight of my research experience. Thank you to Ashley Mason-Burns-Meerschaert and Jay Villemarette (Museum of Osteology), Dr. Alan Resetar and Dr. Adam Ferguson (FMNH), and Katherine Doyle (MNHC) for granting me access to their wonderful collections and providing additional information which made collecting the data for this project an efficient and enjoyable process. I thank my graduate cohort, The Devil Dawgz, and members of the Shimada Lab for providing academic and moral support. Finally, I am indebted to my family and friends for pushing me to pursue my passions and for always being there to listen to me talk about bones and shapes. In particular, a huge thank you to my sister, Catherine Walsh, for numerous R Studio filled sessions. Thank you to all!

Abstract

The relationship between form and function is an overarching theme in the field of biology. Specifically, body size and shape are important factors when considering the biology of an organism. This study examined the torso morphology of a diverse set of 124 extant terrestrial and semi-aquatic amniote taxa using a novel approach to construct approximated torso shape groupings. My study shows the presence of 10 distinct torso shapes within the examined amniotes, and these torso shape groupings were used to evaluate hypotheses associated with diet and limb bone length as well as explore potential evolutionary patterns. Herbivores had a more voluminous torso and were most commonly found to exhibit a torso shape with a wider girth. Also, a statistically significant relationship of certain torso shapes with limb bone lengths was found. These results can be useful for reconstructing extinct taxa. If a relatively complete skeleton is discovered that includes a well-preserved humerus or femur and a torso length is able to be determined, then a torso shape can be approximated using the results of this study. Phylogenetic character mapping identified potential homologous torso shapes in lagomorphs and rodents as well as in artiodactyls and perissodactyls given shared ancestry in these groups. Additionally, potential homoplasious shapes in reptiles and some semi-aquatic mammals were found. This study explored factors that might affect the shape of the amniote torso and provides additional evidence to support that herbivores have large and voluminous torsos to accommodate a gastrointestinal tract needed to digest plant material. Other factors that might influence torso shape include cursoriality, mode of thermoregulation, habitat, life-history, and behavioral or morphological adaptations in response to large scale environmental changes. This study represents a relatively simple and novel approach to investigating a seemingly understudied aspect of the amniote body plan, the shape of the torso.

I. INTRODUCTION

The sizes and shapes of animals have been observed and studied using many different perspectives. Yet, even the earliest physiologists, zoologists, and morphologists identified a possible link between form and function: an overarching theme in the field of biology (Russell, 1916). This theme was explored further in the beginning of the 20th century and morphologists continued to investigate biological processes which impact the growth and form of organisms, combining aspects of developmental biology and embryology in their approach to assess questions associated with form (Russell, 1916; Thompson. 1917). Research in recent years has supplemented this central theme and has introduced newer questions and avenues with which to address the influence of form as it relates to function (Sommerfeldt and Rubin, 2001; Woronowicz and Schneider, 2019; Jones et al., 2020).

Early and current research has determined that body size and form are fundamentally important properties when considering an organism's biology. These morphologically based attributes can have implications on the ecological and physiological traits of an individual. In extant vertebrate taxa, relationships exist between body size and aspects of spatial organization including geographic range size (Arita et al., 1990; Gaston and Blackburn, 1996), abundance (Damuth, 1981; Pyron, 1999), and population size (Swihart et al., 1988). For example, there appears to be an inverse relationship between the size of an animal species and its local abundance (Damuth, 1981). From the physiological standpoint, body size is related to biomechanical functions of vertebrates, especially locomotion (Christiansen, 2002) and an organism's ability to travel long distances more efficiently (Kram and Taylor, 1990). Larger bodied animals, with larger and longer limbs, have been shown to exhibit more efficient and less

energetically costly locomotion (Kram and Taylor, 1990). These relationships associated with body size can also contribute to each organism's ability to withstand changing or extreme environmental conditions (Olden et al., 2007) and are able to impact interspecific interactions (Cohen et al., 1993; Hone and Benton, 2005). Body size and metabolic rates can be considered critical constraints for a given organism's characteristics including behavior and life history (Healy et al., 2013). Ultimately, given a range of implications associated with relationships driven by an individual's morphology, an understanding of animal body size and form becomes important in the context of ecology and evolution of any given species.

Body sizes and shapes have diversified and differentiated at various levels of organismal design. An example of such variation is how the gastrointestinal tract (GIT) is adapted in shape and size to accommodate different diets (Treves, 1886; Stevens and Hume, 1998). In general, herbivores require larger and longer GITs to allow time and space for the microbiota needed to consume difficult to digest plant material (Stevens and Hume, 1998; Clauss et al., 2017). This trend has been demonstrated in certain invertebrate (Griffen and Molsblack, 2011), fish (Wagner et al., 2009), lizard (O'Grady et al., 2005), and mammal (Barry, 1977; Wang et al., 2003) taxa, and at least for herbivorous mammals, the need for digesting plant material has been demonstrated to generally require a more voluminous body cavity (Clauss et al., 2017). Such a relationship between diet and torso volume suggests that there may also be a relationship between diet and the shape of the torso.

Torso morphology, that would have a significant implication for body mass, is considered an indication for diet type in both extant and extinct quadruped taxa (Hotton et al., 1997; Sues and Reisz, 1998). In addition, the length of limb bones (e.g., humeri and femurs) are known to exhibit linear relationships with body mass and thus are commonly used to reconstruct or

approximate aspects of extinct taxa (Campione and Evans, 2012). The torso is also associated with other important physiological traits within amniotes. For example, the ribs and intercostal muscles are integral to locomotion in tetrapods but also play a role in and have influenced the evolution of aspiration breathing in amniotes (Carrier, 1996; Cieri et al., 2020). In addition to the respiratory system, the ribcage and rest of the torso house and protect the viscera and the reproductive systems. Yet, variations of torso morphology among diverse vertebrates, including the shape and its relation to torso volume or body mass, lacks systematic and quantitative investigations throughout the literature (Seebacher, 2001; Clauss et al., 2017). Therefore, the goal of this study is to examine torso shape of diverse extant quadrupedal amniote taxa (i.e., small to large sized, terrestrial and semi-aquatic reptiles and mammals). Specifically, I test the following two hypotheses: 1) "Herbivorous quadrupedal amniotes have a girthier torso for a given body size"; and 2) "There is a relationship between torso shape and limb length in quadrupedal amniotes." If these hypotheses can be supported, my data would provide a new way to infer the torso morphology of extinct quadrupedal amniotes, including non-bipedal dinosaurs that are represented primarily by skeletal remains in the fossil record, because soft tissues are generally not preserved during the fossilization process.

II. MATERIALS AND METHODS

A. EXAMINED SPECIMENS

This study is based on measurements taken from fully or partially mounted articulated skeletal specimens of a diverse set of quadrupedal amniotes, except one preserved specimen in ethanol (Appendix 1). The specimens came from three museum collections in the U.S.: Field Museum of Natural History (FMNH), Chicago, Illinois; Massachusetts Natural History Collections (MNHC), University of Massachusetts, Amherst, Massachusetts; and Museum of Osteology (MoO), Oklahoma City, Oklahoma. For the purpose of this study, I chose to measure specimens with ribs that were in a fixed natural position, maintaining an articulated ribcage. Exactly how they were mounted (e.g., resting, standing, or running posture) or what conditions other parts of the skeleton (e.g., head, neck, or tail) were in had little effect on measurements. In total, I measured 132 skeletal specimens and this resulted in a dataset comprising 124 extant terrestrial and semi-aquatic amniote taxa (Appendix 2), consisting of 24 reptiles (three orders, 12 families, and 17 genera) and 100 mammals (21 orders, 61 families, and 92 genera). In some cases, I measured multiple specimens of the same taxon, and in these cases, I used the average of the torso shape measurements for analyses. The dataset excluded taxa that were fully aquatic and lacked hindlimbs such as cetaceans (whales and dolphins) and sirenians (manatees and dugongs), that had an unconventional torso architecture for tetrapods such as testudines (turtles), or that possessed highly modified forelimbs such as chiropterans (bats).

B. DATA COLLECTION AND TORSO SHAPE CONCEPTUALIZATION

Many quadrupeds exhibit complex body shapes. Complex torso morphology was conceptually simplified to represent two 'elliptic conical frustum' shapes (Fig. 1) defined by nine basic variables: total, anterior, and posterior torso length (TTL, ATL, PTL), maximum torso width and height (MTW, MTH), anterior torso width and height (ATW, ATH), and posterior torso width and height (PTW, PTH). All measurements (Appendix 3) were collected using hand measuring tools (rulers, calipers and tape measures) to the nearest millimeter. TTL was measured as the linear distance from the assumed level of the first paired ribs to the mid-dorsal acetabulum. ATL was the linear distance from the assumed level of the first paired ribs to the widest part of the rib cage. PTL was the calculated difference between TTL and ATL. MTW was the distance between the distal parts of the widest part of the rib cage. MTH was the vertical distance from the top of the head of the rib at the widest point of the rib cage to the top of the most ventral part of the torso. The MTH measurement can vary depending on the preservation of the sternum or costal cartilage of the mounted skeleton. If there was no sternum or costal cartilage preserved, MTH was measured as the vertical distance from the top of the rib at the widest point of the rib cage to an extrapolated ventral surface from the bottom of the longest rib extended. ATW was the linear distance between the most distal points of the first paired ribs. ATH was the vertical height of the first paired ribs. PTW was the linear distance between the junction of the femurs and acetabula. PTH was the vertical height from the ventral side of the pubic symphysis to the most dorsal point of the pelvic bone.

Besides torso morphology, this study examined two additional variables pertaining to forelimbs and hindlimbs in order to elucidate potential relationships and predictive values within

the quadrupedal body plan. Limb measurements included maximum humerus length (MHL) and maximum femur length (MFL). These limb bone measurements were measured as the maximum distance from distal to proximal ends of each respective bone.

The described torso morphology measurements were used to construct two elliptic conical frusta designed to represent the anterior and posterior portions of the torso. The two frusta were constructed separately as an anterior and a posterior frustum and subsequently combined as there was expected variability in anterior and posterior dimensions (Fig. 2). Once combined, these two frusta produced a conceptually simplified model for the complex torso morphology. Simplifying aspects of an individual's morphology is a common practice when estimating body mass using osteological measurements (e.g., Hurlburt, 1999; Seebacher, 2001).

C. DEFINING TORSO SHAPES AND TORSO SHAPE GROUPS

I used *k*-means clustering to determine clusters, or groups, of amniotes based on similarities and differences related to the nine torso shape variables previously described. Prior to clustering, the torso measurements were log-transformed to account for the range of values within the data. Additionally, I corrected for size in the data by generating a ratio with the TTL as the denominator for the remaining eight torso shape variables. From there, I determined the optimal number of clusters, *k*, using the Elbow Method which minimizes the total intra-cluster variation [or total within-cluster sum of square (WSS)]. The Elbow Method represents one of the most commonly used methods for determining an optimal number of clusters and has been shown to be effective in cluster determination (Marutho et al., 2018). In such partitioning methods, the Elbow Method produces a plot (Fig. 3) of a curve that shows the total WSS as a

function of the total number of clusters. The location of a bend ('knee') in the plot marks the point where adding an additional cluster does not significantly impact the total WSS. In my analysis, the bend occurs around group numbers 9–13, but the point where the total group number of 10 was determined to be a reasonable cut-off position because further partitioning would yield additional shapes that would be unnecessarily redundant (see below for the need of 'consolidation' of some torso shapes even with 10 groups). The output from the *k*-means clustering produced average values for the standardized and size-corrected torso shape variables within each group (Table 1), and these values were used to generate an approximate shape for the individuals assigned to each group (Table 2). As *k*-means clustering represents an objective and mathematical approach to partitioning, the clusters, interpreted as torso shape groups, were assessed for biological patterns and in some cases consolidated to account for overlapping permutations of the torso shape variables. The resulting clusters and approximate torso shapes were then used for subsequent analyses to assess the original hypotheses related to the shape of the amniote torso. Subsequent analyses were separated to observe potential patterns across the original and consolidated torso shape groups.

In addition to *k*-means clustering, a Principal Component Analysis (PCA) was used to investigate and visualize potential patterns associated with the shape of the amniote torso. Principal Components (PCs) were also calculated using the log-transformed and size-corrected data described previously. PCA attempts to reduce dimensionality and generates scatter plots which identify the amount of variation each new 'dimension' accounts for as well as how strongly each variable influences the PCs. I conducted *k*-means clustering and PCA using R version 4.0.0 (R Core Team, 2021).

D. VOLUME CALCULATION AND MODEL VALIDATION

Once a conceptualized shape of each individual had been determined, a total volume of each shape was calculated and compared for taxa also examined by Clauss et al. (2017). This comparison was to assess the accuracy of my conceptual model of torso shape. The torso volume (*V*) of each examined specimen was calculated using the equation for the volume of an elliptic conical frustum (Fig. 2) (Vanover, 2014):

$$V = \frac{1}{3}\pi[(ab)H - (cd)(H - h)]$$

Where

$$H = \frac{\sqrt{ab}h}{\sqrt{ab} - \sqrt{cd}} = \frac{ah}{a - c} = \frac{bh}{b - d}$$

In these equations, the variable *H* is calculated first as the elliptic nature of the frusta and each axis of the bases need to be considered. In the equation to determine *H*, *a* always represents the semi-major axis of the large base, *b* the semi-minor axis of the large base, *c* the semi-major axis of the small base, and *d* the semi-minor axis of the small base. *H* is calculated using these same variables as well as *h* which represents the height of the frustum. The measured torso morphology variables were used to calculate the volumes of two elliptic conical frusta which, when combined, represent the total volume of the torso. For the anterior torso volume calculations, *c* was always the longer measurement between ATW and ATH, and *d* was the shorter measurement between ATW and ATH. For posterior torso volume, *c* was the longer measurement between PTW and PTH, whereas *d* was the shorter measurement. For both anterior and posterior torso volume calculations, *a* was always the longer measurement between MTW and MTH, whereas *b* was the shorter of the two measurements. ATL and PTL represent *h* for

their respective frustum calculations. These distinctions allowed for appropriate calculations and accounted for variation in the torso morphology of different amniote taxa.

Once volumes were calculated for each measured specimen, a paired *t*-test was performed on log-transformed data. This was to determine whether there was a significant difference between the mean torso volumes I calculated and the torso volumes reported by Clauss et al. (2017) for respective taxa.

E. DIET TYPE ASSIGNMENT

To assess potential relationships associated with diet, organisms were assigned to one of three diet types: carnivore, herbivore, or omnivore. Species were classified based on the largest proportion of diet items, using a variety of sources (Appendix 4), including a combination of MammalDIET and MammalDIET2 metadata (Kissling et al., 2014; Gainsbury et al., 2017). These datasets represent a compilation of species-specific diet preferences of mammals covering 38% of a total of 5,364 terrestrial mammalian species assessed for the International Union for Conservation of Nature's Red List (Kissling et al., 2014). My dataset comprises 17 carnivores, five herbivores, and two omnivores among the 24 reptile taxa examined, and 39 carnivores, 48 herbivores, and 13 omnivores among the 100 mammal taxa examined (Appendix 4).

F. HYPOTHESIS TESTING

Pearson chi-square tests for independence were used to examine associations between diet type and torso shape. Degrees of freedom for this chi-square test were defined as follows: (r

– 1) × (c – 1), where r = the number of rows and c = the number of columns. Significance level was set at $p < 0.05$.

I conducted a series of statistical tests including the parametric One-way Analysis of Variance (ANOVA) and the non-parametric Kruskal-Wallis H test to compare the effect of limb bone length (MHL and MFL) on torso shape groups. Original and consolidated torso shape groups were separately assessed for normality using a Shapiro-Wilks Test ($p < 0.05$). Depending on the results of the tests for normality, I used ANOVA if the standardized limb bone lengths were normally distributed across torso shape groups, whereas I used Kruskal-Wallis to test groups with non-normal distributions. Post hoc tests were used to further explore which torso shape groups exhibited statistically significant differences. Following the ANOVAs, I used Tukey's honestly significant difference (HSD) post hoc tests, whereas following the Kruskal-Wallis tests, I used Dunn's test. For all tests, significance level was set at 0.05. Data were analyzed using the Real Statistics Resource Pack software (Release 7.6) (Zaiontz, 2021).

G. CHARACTER MAPPING

Phylogenetic character mapping (e.g., Harvey and Pagel, 1991) was used to examine potential evolutionary patterns of torso shapes within amniotes. The torso shape groupings were mapped for the taxa represented in this study on a tree generated using the National Center for Biotechnology Information (NCBI) Common Tree online tool based on the NCBI taxonomy database (Schoch et al., 2020). This database is derived from a diverse array of phylogenetic resources and produced a simplified molecular-based phylogenetic tree that included only the taxa measured as a part of this study. The trees generated using this tool represent graphically

presentable trees that are not strictly phylogenetic; however, I compared those trees with previously published molecular-based phylogenetic trees for both mammals and reptiles to confirm the congruency in tree topology (e.g., Delsuc et al., 2002; Flynn et al., 2005; Springer et al., 2004; Green et al., 2014; Simões et al., 2018). The use of molecular-based trees, rather than morphology-based trees, for my character mapping is deliberate because the torso morphology is completely independent of the construction of those molecular-based trees.

III. RESULTS

A. Model Validation Results

A paired *t*-test was conducted on a sample of 20 measured amniotes (17 mammals and three reptiles) which overlapped between my dataset and those reported from Clauss et al. (2017). The goal of this *t*-test was to determine whether there was a statistically significant mean difference between the torso volumes (cm^3) calculated using my torso shape model (Fig. 1) compared to the volumes of the same species as reported by Clauss et al. (2017). Both sets of volumetric data were log-transformed to account for large variation in the values. Figure 4 depicts a graph with plots of the standardized average torso volumes calculated for the 20 amniote taxa based on each of the two methods, where each plot pair for the same taxon is connected with a line. The slopes of the lines in Figure 4 show that my method generally gives a slightly underestimated torso volume than Clauss et al.'s (2017) method with a few exceptions, but my *t*-test [i.e., ($\bar{x}$ = 4.15, *SD* = 0.95), $t(19) = -1.56$, $p = 0.06$] indicated that there was no significant difference in mean torso volumes calculated from my shape model ($\bar{x}$ = 4.03, *SD* = 1.07) and from those based on the digital convex hull method used by Clauss et al. (2017).

B. Torso Shape Groupings

The results of the Elbow Method suggest that the optimal number of clusters (*k*) is 10 as the curve of Total WSS according to the number of clusters *k* shows a bend at 10 clusters (Fig. 3). Therefore, the final *k*-means clustering analysis was performed, and results were extracted with $k = 10$.

My *k*-means clustering using the standardized and size-corrected eight torso shape variables yielded ten groups containing a range of 1 to 27 individuals. The cluster assignments are summarized in Table 2. Also extracted from the *k*-means clustering were the cluster centers, or means, for the ten groups across the eight torso shape variables. These center values are summarized in Table 1 and were used to generate torso shape approximations shown in Figure 5.

Based on differences between the anterior, posterior, and maximum lengths, widths, and heights, I identified and approximated the shape of the torso for the members within a given group. Upon further review, the center values for groups 1 and 10 shared the same overall torso 'shape' (a short and wide anterior torso with a long, wide posterior torso and MTW greater than MTH). Given the observed similarities between groups 1 and 10 as well as similarities between groups 6 and 7, I opted to consolidate these pairs of torso shape groups to generate a total of eight torso shape groups. Additionally, the *k*-means clustering algorithm assigned a single taxon to group 2, the chameleon. For reasons described in further detail below, I removed group 2 from the dataset, resulting in just seven total torso shapes. The remaining analyses to assess relationships associated with the shape of the amniote torso used these three configurations and torso shape groupings were analyzed separately. These groupings are displayed in Figure 6, where the original 10 torso shape groups are coded by color. The scatterplot of the PCA coded for torso shape groupings (Fig. 6) shows that the groupings determined by PCA are consistent with the results from *k*-means clustering. There are distinct clusters based on torso shape present in the scatterplot. This consistency helps to demonstrate that the groupings determined by *k*-means are robust.

Figure 6 shows a PCA scatter plot that is displayed using the first two principal component axes (PC1 and PC2) that accounted for 75.58% of the variation within the dataset.

The color-coding scheme was determined using the original ten torso shape groups assigned by *k*-means clustering (Table 2). This plot of the relationship between PC1 and PC2 highlights some of the patterns associated with the shape of the amniote torso. Of note is the clustering of torso shape groups 8 and 10 which are shapes most commonly seen in reptiles measured in this study. These torso shape groups occupy the upper portion of the morphospace due to the exceptionally wide torsos seen in many of the reptiles measured in this study, including the gharial and Yacare caiman. The cluster that represents torso shape group 5 occupies the right-most region of the morphospace and these animals have both tall and wide torsos, especially the African elephant and giraffe.

C. Principal Component Analysis

Appendix 5 shows my raw coordinate data from PCA. PCA revealed that the first two dimensions, or principal component axes, account for 75.58% of the variation in the data. The first dimension, which explains 64.79% of the variation, exhibited large positive associations with PTW, PTH, ATH, and ATW. The second dimension, which explains 10.70% of the variation, had a positive association with ATL and a negative association with PTL. Together, these two axes account for a large portion of the variation and appear to account for differences in general torso shape separated between anterior and posterior torsos. Appendix 6 shows the loadings of each torso shape variable for the first two dimensions. Scatter plots were generated to examine potential groupings based on both diet and taxonomic relationships with the loadings of each torso shape variable overlaid (Figs. 7, 8).

The scatterplot that displays the torso shape groupings coded by diet (Fig. 7) shows a relatively wide distribution and identifies a few potential patterns. In general, herbivores (green)

appear to clump on the right side of the morphospace due to their ‘girthy’ torsos that exhibit large height and width measurements. The carnivores (red) do not exhibit as much of a clear pattern, and omnivores (blue) also appear to be spread throughout the morphospace. Figure 8, a scatterplot coded by taxonomic relationship at the class rank, displays a major division between the reptiles (red) and mammals (blue) measured in this study. As described above, reptiles generally exhibit a wide overall torso shape that places them primarily in the upper portion of the morphospace. On the other hand, mammals exhibit more variation in the shape of the torso.

D. Effects of Diet on Torso Shape

Three separate chi-square tests of independence were performed to examine the relationship between diet and torso shape. The first test examined the original ten torso shape groups determined by *k*-means clustering and found that there is not enough evidence to conclude that these variables are associated, $x^2(18, n = 124) = 25.49$, $p > 0.05$. The second test examining the consolidated groups of eight total torso shapes yielded similar results and failed to reject the hypothesis that diet and torso shape are associated, $x^2(14, n = 124) = 23.40$, $p > 0.05$. The third test with consolidated torso shape groups and the chameleon removed demonstrated that the relationship between diet and torso shape was in fact significant, $x^2(12, n = 123) = 22.25$, $p < 0.05$. The distributions of each diet type as a function of the final consolidated seven torso shape groupings are shown in Figure 9.

Figure 9A shows the distribution of torso shape groups for the herbivores ($n = 48$) measured in this study. The combined group of torso shapes 6 and 7 is the most abundant with 14 individuals followed by torso shape groups 3 and 4 with 12 and 11 individuals respectively. The distribution of carnivores ($n = 59$, Fig. 9B) demonstrates that the combined group of torso

shapes 1 and 10 is the most abundant with 14 individuals followed by the combined group of torso shapes 6 and 7 with 13 individuals. Lastly, Figure 9C shows the distribution of organisms classified as omnivores (n = 16). Torso shape 4 is the most common, with six omnivores exhibiting this torso shape.

E. Effects of Limb Bone Length on Torso Shape

a. Effects of Humerus Length on Torso Shape

To test the effects of maximum humerus length (MHL) on torso shape, I first used Shapiro-Wilks tests to assess the normality of the distribution of standardized humerus values across the three torso shape groupings: 1) the original ten torso shapes, 2) the eight torso shapes after the first round of consolidation, and 3) the seven torso shapes after the removal of the chameleon. All three tests revealed non-normal distributions ($p < 0.05$) within the torso shape groups. Torso shape 3 exhibited non-normal distributions in each case as did the consolidated shape of 1 + 10. Based on the results of these Shapiro-Wilks tests, I opted to use a Kruskal-Wallis H test to test the null hypothesis that there is no difference in MHL values across torso shape groups determined by k-means clustering. The independent variables were the assigned torso shape groups and the dependent variable was the log-transformed and size-corrected MHL values. Tables 3 and 4 show the mean standardized MHL values and standard errors for the original and consolidated torso shape groupings.

The Kruskal-Wallis test of MHL for the original ten torso shapes revealed a statistically significant difference in mean MHL between the torso shape groups, $H(9) = 70.26$, $p < 0.05$. Results of post hoc comparisons using Dunn's test are summarized in Table 5 and indicate which torso shapes differed significantly. When consolidated to eight torso shape groups, their Kruskal-

Wallis test of MHL also showed that MHL values affects torso shape grouping, $H(7) = 68.54$, $p < 0.05$. Post hoc comparisons and significant differences between groups are summarized in Table 6. The third Kruskal-Wallis test also demonstrated statistically significant differences, $H(6) = 66.8$, $p < 0.05$ and the post hoc results from the third Dunn's test can be found in Table 7.

b. Effects of Femur Length on Torso Shape

Starting with the original ten torso shape groupings (Fig. 5), a set of Shapiro-Wilks tests were used to assess the normality of the distribution of log-transformed and size-corrected values of maximum femur length (MFL) across these torso shape groupings. Results of the first test with the original ten torso shapes indicated that MFL values for each of the torso shape groups were normally distributed ($p > 0.05$) except for groups with a single representative: torso shape groups 2 and 6 representing the chameleon and black lemur, respectively. Following the first round of consolidation down to eight torso shapes, a second Shapiro-Wilks test indicated normality ($p > 0.05$) across all groups besides torso shape group 2, the single chameleon. A final round of consolidation, which removed the chameleon, and subsequent Shapiro-Wilks test demonstrated once again that the MFL values for these seven torso shape groups were normally distributed ($p > 0.05$).

Three separate One-way Analysis of Variance (ANOVA) tests were used to examine whether MFL is a function of the torso shape group determined by *k*-means clustering. Multiple ANOVAs were used to examine the relationships in the original ten torso shape groupings as well as the groupings determined following the consolidation of similar shapes and removal of outlier shapes. The independent variables were the assigned torso shape groups and the dependent variable was the log-transformed and size-corrected MFL values. Tables 3 and 4 show

the mean standardized MFL values and standard errors for the original and consolidated torso shape groupings.

The One-way ANOVA of MFL for the original ten torso shapes (Table 8) revealed a statistically significant main effect, $F(9, 114) = 22.5$, $p < 0.05$, indicating that not all ten torso shape groups had the same MFL. Post hoc comparisons using Tukey's honestly significant difference procedures (HSD) were used to determine which pairs of the ten torso shapes were significantly different. These results are summarized in Table 9 and indicate several significantly different MFL values across torso shapes. When consolidated to eight torso shape groups, their One-way ANOVA of MFL (Table 10) also revealed a significant main effect, $F(7, 116) = 23.2$, $p < 0.05$. Post hoc comparisons yielded significant differences between several torso shape groups as well and these results are summarized in Table 11. The third One-way ANOVA of MFL in the seven torso shape groups (Table 12) revealed a statistically significant main effect, $F(6, 116) = 25.8$, $p < 0.05$. Table 13 summarizes which of the final seven torso shape groups demonstrated significantly different mean MFL values following Tukey's HSD post hoc comparisons.

F. Character Mapping

I used simplified versions of previously published molecular-based phylogenetic trees to examine the evolutionary patterns in torso shape within the amniote clades through character mapping. Based on the ten initial torso shape groupings determined by *k*-means clustering, the reptiles (Fig. 11) exhibited six different torso shapes with the most common being shapes 8 and 10, with ten individuals each. When consolidated, the most common shape becomes the combination of shapes 1 and 10, with eleven total reptiles sharing this torso shape. Members of the order Crocodylia were either shape 8 or 10 whereas the remaining reptiles of the superorder

Lepidosauria, including the Squamates and *Sphenodon*, contained individuals with other shapes as well.

Within the class Mammalia, the monotremes (Monotremata) and marsupials (Marsupialia) represent the most basal clades I measured. Five representatives (Fig. 12) of these two sister clades were measured and represented four different torso shapes, with the echidna and wallaby sharing the same shape 3. Five taxa of the clade Afrotheria (Fig. 12) were measured and exhibit three different shapes: shapes 3, 4 and 5. The afroinsectivorans, a clade within Afrotheria, measured in this study (elephant shrew and tenrec) shared the same shape 4. Sister to the Afrotheria are the xenarthrans (Fig. 12) that share the same three shapes exhibited in the afrotherians. The next most derived clade and superorder is the Euarchontoglires (Fig. 13), the living members of which belong to one of the following five groups: colugos, treeshrews, primates, lagomorphs, and rodents. Within this superorder, six shapes are represented: shapes 3, 4, 5, 6, 7, and 10. Just five are present when the single member of shape 6 (black lemur) is consolidated to shape 7. Shape 4 is the most common shape exhibited in this superorder and is shared by 13 members, including the one member of Dermoptera, three primates, two lagomorphs, and seven rodents. The final clade and superorder, Laurasiatheria (Fig. 14), is also the largest based on the examined taxa and contained 59 individuals representing seven different original shapes (1, 3, 4, 5, 7, 9, and 10) and six when shapes 1 and 10 are consolidated. In both cases, shape 7 is the most common with 23 individuals followed by shape 3 with 12. Within this superorder is the clade Euungulata, containing the groups Perrisodactyla and Artiodactyla. The 20 ungulates measured in this study have one of three shapes: 3, 5 or 7. The perrisodactyls (horse, rhinoceros, and tapir) all shared shape 5. Also within Laurasiatheria are the carnivorans (Fig. 15) and this order represents the largest group measured within this study with 35

individuals. Fifteen of these individuals exhibit shape 7, including six of eight canids and two of four felids, representing the most common shape of the carnivorans.

IV. DISCUSSION

A. A novel method for investigating the amniote torso

Based on my results and subsequent comparisons to results reported in Clauss et al. (2017), the method proposed in this study represents a reasonable alternative approach for investigating patterns associated with the amniote torso. It also represents a simplified method that does not require sophisticated three-dimensional, computer-based modeling employed by Clauss et al. (2017). Hand measurements of the nine torso shape variables were sufficient to construct an approximation of the torso shape of a given individual and this approximation served as an effective model for further analyses. Three-dimensional models and reconstructions have become popular in similar studies (Mallison, 2010; Sellers et al., 2012; Clauss et al., 2017). Yet, these methods require access to software and hardware that can be limiting. This study demonstrates a novel, more accessible approach to investigating the amniote torso morphology.

B. Relationships associated with the shape of the amniote torso and their significance

The hypothesis that herbivores have a more voluminous or girthy torso shape is supported by the results of the third chi-square test of independence demonstrating a significant relationship between diet and torso shape ($p < 0.05$). Herbivores are most abundant in torso shapes 3, 4 and 7 with 12, 11 and 14 representatives, respectively (Fig 9A). Individuals within torso shape 3 possess a MTW greater than MTH. Torso shape 4 individuals have greater ATW and MTW relative to ATH and MTH. Lastly, torso shape 7 is categorized by a PTW greater than PTH. The three most common shapes within the herbivores represent shapes with ratios that can be interpreted as possessing a girthy torso. Additionally, within the dataset, herbivores have the largest average standardized volume when compared to carnivores and omnivores (Fig. 10).

The second hypothesis that there exists a relationship between torso shape and limb bone length is also supported based on the results of the series of ANOVA and Kruskal-Wallis tests as well as the associated post-hoc tests. The ANOVA and Kruskal-Wallis tests for the original and both consolidated torso shape groups show significant main effects ($p < 0.05$), indicating significant differences in MHL and MFL between and amongst the torso shapes.

The results of my hypothesis testing are significant from the standpoint of vertebrate paleontology. For example, limb bones are frequently used to estimate aspects of the biology of extinct taxa, and these results may allow for further estimations and reconstructions of the shape of the torso for extinct forms. Given a certain limb bone length and a determinable total torso length of an extinct individual which fits the parameters of the focal taxa for this study, that individual could be placed in one or more torso shape groups depending on those measurements. For example, a ceratopsian dinosaur *Pentaceratops sternbergi* (Ornithischia) is reported to have a femur length of approximately 1,000 mm and a TTL of about 4,100 mm (Lehman, 1998). When log transformed and corrected for size with TTL as the denominator, this ceratopsian dinosaur has a MFL that falls within the same range of MFL values found in torso shapes 4 and the combined group of shapes 6 and 7. Based on the post hoc analyses, there were no significant differences between the average MFL values for these two groups, so *P. sternbergi* could therefore exhibit either shape according to my results. Because much of the fossil record of non-avian dinosaurs is based on incomplete specimens (e.g., Dodson, 1990; Benton et al., 2011) the fact that my study can narrow down the possible torso shapes of extinct taxa from the limb length alone is significant.

C. Evolutionary patterns of amniote torso shape

Evolutionary patterns of torso shape based on character mapping are most apparent within the reptiles. Shapes 8 and 10 are most abundant in these groups and are the only shapes present within the order Crocodylia (Fig. 11). Individuals within these two torso shape groups exhibit torsos that are universally wider than they are tall with the only difference being the length of the anterior or posterior torso. Many extant reptiles, including crocodylians and lepidosaurs, are known for their wide torsos, and it is possible that this feature comes from the shared ancestry of these groups. Ectothermy is a trait seen in reptiles, and although there are behavioral adaptations which impact thermal regulation in these animals, an increased surface area defined by wider and longer torsos may also impact a reptile's ability to regulate its body temperature without affecting its metabolic rate.

My study shows that there is more variation of torso shapes within the mammals, and with more variation, there are fewer discernable patterns. Nevertheless, certain groups share the same torso shapes, and this may be evidence for certain torso shapes as either homologies or homoplasies. Of note are the three perissodactyls (horse, rhinoceros, and tapir) measured as a part of this study sharing torso shape 5 (Fig. 14). This shape is also seen in a number of large herbivorous mammals including the elephant, giraffe, bison, and hippopotamus amongst others. This shape exhibits a longer MTW than MTH but longer heights in the anterior and posterior torso regions. Within the rodents, seven of twelve measured as a part of this study possess torso shape 4, and this shape is also present in the sister group, the lagomorphs.

The examples described above can be interpreted to be potential homologies based on the positions of these groups on the phylogenetic trees (Figs. 13, 14). In both examples, the pairs of closely related groups (rodents and lagomorphs as well as perissodactyls and several

artiodactyls) exhibit similar or identical torso shapes (i.e., torso shapes 4 and 5 respectively), suggesting that the shape of the torso was derived from a common ancestry. On the other hand, there are examples of similar or identical torso shapes in taxa that are not closely related according to my character mapping. For example, torso shape 10 is most commonly seen in reptiles (Fig. 11), yet there are a few mammals that share this torso shape (e.g., platypus, sea lion and monk seal). In this case, the shape of the torso can be interpreted as a potential homoplasy.

The reptiles measured in this study are represented by one of two clades: Lepidosauria and Crocodylia. Lepidosauria can be further separated into Rhynchocephalia and Squamata. Rhynchocephalia is currently represented by a single surviving genus, *Sphenodon*, and this genus represents the most 'ancestral' reptile examined in this study (Evans, 2009). Within squamates, a sister group to Rhynchocephalia, is the clade Iguania (iguanas, chameleons, and agamas). In this study, this group is represented by the green iguana, desert iguana, Fischer's chameleon, Bearded dragon, and Egyptian mastigure. Within these basal reptile groups, torso shape 10 is the most abundant and is shared by *Sphenodon* and members of Iguania, suggesting that this torso shape may be the ancestral state, whereas the other most abundant torso shape 8 may represent a more derived state.

Living mammals fall into three major groups: Monotremata, Marsupialia, and Eutheria. Of these three groups, the egg-laying monotremes are most basal followed by the pouched marsupials (Upham et al., 2019). Within the more diverse placentals (Eutheria), there exists some uncertainty as to which group represents the most basal lineage (Evans, 2009). Morphological data suggest that it is Xenarthra (sloths, armadillos, anteaters) but molecular studies identify Afrotheria (elephants, elephant shrews, tenrecs, aardvarks) as the most basal lineage (Asher et al., 2003). Nevertheless, the most common torso shape group across all of these

groups is torso shape 3 and is present in one of the most basal monotremes, represented by the short-nosed echidna (Fig. 12). Due to its prevalence in the more basal mammalian groups, torso shape 3 may represent a more ancestral state in regard to the shape of the torso for mammals.

D. Factors that could influence torso shape

There are a number of factors which may influence the shape of an individual's torso. This study explored the relationships between diet and torso shape and found evidence to support that a larger and more voluminous torso in herbivores is likely associated with a larger body cavity to accommodate lengthy alimentary canals thus increasing the capacity for digesting plant material (Clauss et al., 2017). There may be other factors that could impact the shape of an individual's torso. One such factor includes locomotion wherein the shape and size of the torso may limit the cursoriality of an animal (Bramble, 1987). Locomotion may also influence an animal's ability to capture or evade prey and can serve as a selective pressure for an adaptation towards a certain body shape. Interspecific competition has been shown to drive the evolution of certain morphological traits in bivalves and gastropods (West et al., 1991), and this may also apply to the groups examined in this study. Herbivores, both extant and extinct, may have adapted to grow larger in size to avoid predation. Conversely, others may have adapted other body forms to evade predation, such as smaller and thinner bodies ideal for hiding or burrowing which may point to a shared torso shape in the rodents and lagomorphs. Carnivorous animals may have also developed certain body shapes in order to more effectively obtain prey, such as the elongate bodies of weasels to capture burrowing prey (Brown and Lasiewski 1972). This idea of an 'evolutionary arms race' has suggested that prey species are more heavily impacted by selective pressures imposed by predators (Abrams, 1989; Vermeij, 1994; Brodie and Brodie,

1999). Therefore, phenotypic changes, including changes to the shape and size of the torso, may evolve in response to predation.

Evolutionary shifts in body size and shape can be attributed to a response to shifts in environmental conditions which can change adaptive zones and allow for proliferation of new body forms in response to new available niches (Law, 2019). As discussed above, thermoregulation in mammals and reptiles may also affect torso shape and can be considered a limiting factor on torso shape. Ectotherms rely on their environment to regulate internal body temperature and thus are generally confined to warmer environments. The results of this study demonstrate that some reptiles (e.g., tuatara, green iguana and bearded dragon) share similar torso shapes which may be related to their ability to thermoregulate. Whereas torso shape patterns in mammals appear to be less discernable, studies related to Bergmann's rule (Ashton and Feldman, 2003; Porter and Kearney 2009) suggest that increased endotherm (and some ectotherm) body size is associated with an increased latitude and decreasing environmental temperature as larger endothermic bodies conserve heat better. Many of the larger animals included in this study exhibited similar body shapes, so perhaps both size and shape are also related to an animal's ability to thermoregulate.

Habitat and lifestyle may also play a role in an animal's torso shape. This study included semi-aquatic amniotes, and results indicate that there may be a particular shape associated with animals adapted for life in the water. Torso shape 10 is more common in reptiles but is also found in three mammals: the platypus, sea lion, and monk seal. These semi-aquatic mammals exhibit a 'reptilian' torso shape of longer anterior, maximum, and posterior widths. Also found within this group were several crocodilians, suggesting that this particular body shape may represent a homoplasy associated with a more aquatic lifestyle. Another example is with the

chameleon that represented the only case of torso shape 2. Chameleons are the only truly arboreal reptiles and as such exhibit unique adaptations which allow for ‘arboreal locomotion’ (Fischer et al., 2010). This unique mode of travel on branches with small diameters has led to morphological and behavioral modifications especially within the limbs and axial motion, potentially explaining the assignment of the chameleon in its own torso shape group. These unique characteristics of the chameleon and subsequent unique torso shape assignment influenced the decision to omit it from some of the analyses described above.

Another limit to consider related to the torso shape is reproductive biology and life-history in that the size, frequency, and type of life-history may be constrained by the size and shape of an individual. The physical size of each neonate or egg as well as general litter or clutch size may also serve as a limiting factor for torso shape. Larger individuals tend to have larger offspring, and this represents a tradeoff as body size has been shown to be negatively correlated with litter size, breeding frequency, and the total number of offspring per year in terrestrial mammals (Janis and Carrano, 1992). These tradeoffs are not present in terrestrial non-passerine birds and that has been extended to non-avian dinosaurs, suggesting that the reproductive strategies of large terrestrial dinosaurs may have influenced their long-term evolutionary success (Janis and Carrano, 1992; Werner and Griebeler, 2011). Body size appears to play a role in the reproductive strategies and success of certain taxa, and as stated above these patterns may also extend to the shape of the amniote torso. Taxa of similar sizes measured in this study share a similar torso shape as demonstrated by the perissodactyls and other large herbivorous mammals as well as rodents and lagomorphs sharing similar shapes. These similarities may also reflect a connection between these shapes and similar reproductive strategies.

E. Potential future research

Based on the approach of Clauss et al. (2017), this study explored the known general relationship between body size and limb length (Campione and Evans, 2012) as it relates to the shape of the torso. An additional measurement of the circumferences of the femur and humerus may be worth investigating in the future as this body size-limb bone relationship is also considered robust (Anderson et al., 1985). There also exist variations in skeletal structures present in certain groups, such as gastralia in crocodilians and tuatara. This study focused on the skeletal anatomy of amniotes but to gain potential additional insights into the amniote *bauplan*, future studies may consider the use of taxidermic specimens or even live animals. Another consideration was limited access to collections with skeletal specimens and the available information for each specimen. For example, differences in sex may be explored in the future as there may exist variation in the torso related to factors such as sexual dimorphism. Additionally, exploring potential scaling relationships associated with the shape of the amniote torso is worth considering as other parts and physiological aspects of living organisms exhibit differential growth rates. Nevertheless, my study represents a novel approach to investigating the shape of the amniote torso and provides additional insights that can supplement the current knowledge presented in studies such as Clauss et al. (2017).

V. CONCLUSIONS

The relationship between form and function is an overarching theme in the field of biology. Specifically, body size and shape are important factors when considering the biology of an organism. An organism's morphology can influence its ecology and physiology and body size is related to a number of different ecological and physiological aspects for a given organism. This study examined the torso morphology of a diverse set of 124 extant terrestrial and semi-aquatic amniote taxa using a novel approach to construct approximated torso shape groupings in order to evaluate hypotheses associated with diet and limb bone length. These groups were also used to explore potential evolutionary patterns related to the shape of the amniote torso.

Measurements of fully or partially mounted and mostly articulated skeletal specimens from several museum collections were used for this study. These measurements represented nine torso shape variables that combined to produce a simplified conceptual model of the amniote torso. Besides the torso, limb bone measurements were also collected to explore potential relationships associated with the limbs and the shape of the torso. These conceptualized torso shapes allowed me to calculate a volume of the torso using the measured torso shape variables, and I compared these volumes to those of the same taxa previously published in order to evaluate the accuracy of my conceptualized torso shape model. I used partitioning and dimension reducing techniques, including *k*-means clustering and PCA, to assign individuals to torso shape groups. Once determined, these groups were used to assess the hypotheses for this study. I also assigned individuals to one of three diet types: carnivore, herbivore, or omnivore. This allowed me to assess potential relationships associated with diet. Additionally, statistical tests including Pearson chi-square tests for independence, ANOVA, and Kruskal-Wallis tests were used to

evaluate the hypotheses associated with diet and limb bone length. Finally, character mapping allowed me to examine potential evolutionary patterns of torso shapes within amniotes.

The proposed method for approximating the torso shape of a given individual yielded promising results as the torso volume calculated using my method did not statistically differ from a previously published method (i.e., study by Clauss et al., 2017). *K*-means clustering determined that 10 distinct torso shapes were represented within the dataset. However, within these 10 shapes, there were shapes that exhibited identical ratios of heights, widths, and lengths, and were therefore consolidated to seven total torso shapes across the measured taxa. These groups were used to evaluate the hypotheses presented within this study.

The first hypothesis that there is a relationship between diet and torso shape was supported based on the results of chi-square tests of independence which determined that there is a statistically significant difference between observed and expected values for diet types within a given torso shape. On average, herbivores had a more voluminous torso and were most commonly found to possess a torso shape with a wider girth. The second hypothesis that there is a relationship between torso shape and limb bone lengths was also supported as results from several ANOVA and Kruskal-Wallis tests demonstrated statistically significant main effects and subsequent post-hoc analyses indicated different mean femur and humerus lengths between certain torso groups. These results can be useful for reconstructing extinct taxa. If a relatively complete skeleton is discovered that includes a well-preserved femur and or humerus and a torso length is able to be determined, the results of my study can facilitate the reconstruction of fossil quadrupeds. Character mapping identified similar torso shapes within the examined reptiles as well as within some select mammalian groups. I identified potential torso shapes that could be considered homologies and homoplasies based on the evolutionary relationships presented within

this study. Examined lagomorphs, including the European rabbit and Collared pika, share torso shape 4 with several rodents, such as both examined members of the Cricetidae (muskrat and Round-tailed muskrat) as well as the North American and Mountain beavers, amongst others. I was also able to suggest likely ancestral and derived states of the shape of the amniote torso. For reptiles, torso shape 10 appears to be ancestral because it is seen most commonly in basal groups (e.g., Rhynchocephalia and members of the clade Iguania) whereas torso shape 8 is presented as a more derived torso shape seen in more derived groups. Torso shape 3 represents a theoretical ancestral state in mammals due to its prevalence in basal mammalian groups (Monotremata, Marsupiala, Xenarthra and Afrotheria).

This study explored factors that may affect the shape of the amniote torso and provides additional evidence to support that herbivores have large and voluminous torsos to accommodate a GIT needed to digest plant material. Other factors that may influence torso shape include cursoriality, mode of thermoregulation, habitat, life-history, and behavioral or morphological adaptations in response to large scale environmental changes. Previous studies explored aspects of the amniote torso, including volume (Clauss et al., 2017), yet this study represents the first to quantitatively investigate the shape of the amniote torso. Exploring shape provides additional insights for the overall biology of a given organism and this study can contribute to the existing knowledge as it pertains to a fundamental theme in biology: the interplay between form and function. In conclusion, this study represents a relatively simple and novel approach to investigating a seemingly understudied aspect of the amniote body plan, the shape of the torso. The model constructed using this approach can be used to infer and further explore potential relationships within extant taxa and can provide insights into similar relationships of extinct taxa as well.

LITERATURE CITED

Abrams, P. A. 1986. Adaptive responses of predators to prey and prey to predators: the failure of the arms-race analogy. Evolution 40:1229–1247.

Anderson, J. F., A. Hall-Martin, and D. A. Russell. 1985. Long-bone circumference and weight in mammals, birds and dinosaurs. Journal of Zoology 207:53–61.

Arita, H. T., J. G. Robinson, and K. H. Redford. 1990. Rarity in neotropical forest mammals and its ecological correlates. Conservation Biology 4:181–192.

Asher, R., M. Novacek, and J. Geisler. 2003. Relationships of endemic African mammals and their fossil relatives based on morphological and molecular evidence. Journal of Mammalian Evolution 10:131–194.

Ashton, K. G., and C. R. Feldman. 2003. Bergmann's rule in nonavian reptiles: turtles follow it, lizards and snakes reverse it. Evolution 57:1151–1163.

Barry, R. E. 1977. Length and absorptive surface area apportionment of segments of the hindgut for eight species of small mammals. Journal of Mammalogy 58:419–420.

Beck, D. D. 1990. Ecology and behavior of the Gila monster in southwestern Utah. Journal of Herpetology 24:54–68.

Benton, M. J., A. Dunhill, G. T. Lloyd, and F. G. Marx. 2011. Assessing the quality of the fossil record: insights from vertebrates. Geological Society of London Special Publications 358:63–94.

Bramble, D. M. 1987. Cursorial specialization of the mammalian thorax. American Zoologist 27, 87A.

Brodie, E. D., III, and E. D. Brodie, Jr. 1999. Predator-prey arms races: asymmetrical selection on predators and prey may be reduced when prey are dangerous. BioScience 49:557–568.

Brown, J. H., and R. C. Lasiewski. 1972. Metabolism of weasels: the cost of being long and thin. Ecology 53:939–943

Campione, N. E., and D. C. Evans. 2012. A universal scaling relationship between body mass and proximal limb bone dimensions in quadrupedal terrestrial tetrapods. BMC Biology 10, 60. doi: 10.1186/1741-7007-10-60.

Carrier, D. R. 1996. Function of the intercostal muscles in trotting dogs: ventilation or locomotion? Journal of Experimental Biology 199:1455–1465.

Cartland-Shaw, L. K., A. Cree, C. M. Skeaff, and N. M. Grimmond. 1998. Differences in dietary and plasma fatty acids between wild and captive populations of a rare reptile, the tuatara (*Sphenodon punctatus*). Journal of Comparative Physiology B 168:569–580.

Christiansen, P. 2002. Locomotion in terrestrial mammals: the influence of body mass, limb length and bone proportions on speed. Zoological Journal of the Linnean Society 136:685-714.

Cieri, R. L., S. T. Hatch, J. G. Capano, and E. L. Brainerd. 2020. Locomotor rib kinematics in two species of lizards and a new hypothesis for the evolution of aspiration breathing in amniotes. Scientific Reports 10:7739. doi: 10.1038/s41598-020-64140-y.

Clauss, M., I. Nurutdinova, C. Meloro, H. Gunga, D. Jiang, J. Koller, B. Herkner, P. M. Sander, and O. Hellwich. 2017. Reconstruction of body cavity volume in terrestrial tetrapods. Journal of Anatomy 230:325–336.

Cohen, J. E., S. L. Pimm, P. Yodzis, and J. Saldaña. 1993. Body sizes of animal predators and animal prey in food webs. Journal of Animal Ecology 62:67–78.

Damuth, J. 1981. Population density and body size in mammals. Nature 290:699–700.

da Silva, J. M., L. Carne, G. J. Measey, A. Herrel, and K. A. Tolley. 2016. The relationship between cranial morphology, bite performance, diet and habitat in a radiation of dwarf chameleon (*Bradypodion*). Biological Journal of the Linnean Society 119:52–67.

Delsuc, F., M. Scally, O. Madsen, M. J. Stanhope, W. W. de Jong, F. M. Catzeflis, M. S. Springer, and E. J. P. Douzery. 2002. Molecular phylogeny of living Xenarthrans and the impact of character and taxon sampling on the placental tree rooting. Molecular Biology and Evolution 19:1656–1671.

Dodson, P. 1990. Counting dinosaurs: how many kinds were there? Proceedings of the National Academy of Sciences 87:7608–7612.

Engeman, R. M., B. W. Kaiser, and K. J. Osorio. 2019. Evaluating methods to detect and monitor populations of a large invasive lizard: the Argentine giant tegu. Environmental Science and Pollution Research 26:31717–31729.

Erickson, G. M., P. M. Gignac, S. J. Steppan, A. K. Lappin, K. A. Vliet, J. D. Brueggen, B. D. Inouye, D. Kledzik, and G. J. W. Webb. 2012. Insights into the ecology and evolutionary success of crocodilians revealed through bite-force and tooth-pressure experimentation. PLoS ONE 7:e31781. doi: 10.1371/journal.pone.0031781.

Evans, S. E. 2009. Evolution and phylogeny of amniotes; pp. 1192–1194 in M. D. Binder, N. Hirokawa, and U. Windhorst (eds.), Encyclopedia of Neuroscience. Springer Berlin Heidelberg, Berlin, Heidelberg.

Faurby, S., M. Davis, R. Ø. Pedersen, S. D. Schowanek, A. Antonelli1, and J.-C. Svenning. 2018. PHYLACINE 1.2: the phylogenetic atlas of mammal macroecology. Ecology 99:2626

Fischer, M. S., C. Krause, and K. E. Lilje. 2010. Evolution of chameleon locomotion, or how to become arboreal as a reptile. Zoology 113:67–74.

Flynn, J. J., J. A. Finarelli, S. Zehr, J. Hsu, and M. A. Nedbal. 2005. Molecular phylogeny of the Carnivora (Mammalia): Assessing the impact of increased sampling on resolving enigmatic relationships. Systematic Biology 54:317–337.

Gainsbury, A. M., O. J. S. Tallowin, and S. Meiri. 2018. An updated global data set for diet preferences in terrestrial mammals: testing the validity of extrapolation. Mammal Review 48:160–167.

Gaston, K. J., and T. M. Blackburn. 1996. Conservation implications of geographic range size-body size relationships. Conservation Biology 10:638–646.

Green, R. E., E. L. Braun, J. Armstrong, D. Earl, N. Nguyen, G. Hickey, M. W. Vandewege, J. A. St John, S. Capella-Gutiérrez, T. A. Castoe, C. Kern, M. K. Fujita, J. C. Opazo, J. Jurka, K. K. Kojima, J. Caballero, R. M. Hubley, A. F. Smit, R. N. Platt, C. A. Lavoie, M. P. Ramakodi, J. W. Finger, A. Suh, S. R. Isberg, L. Miles, A. Y. Chong, W. Jaratlerdsiri, J. Gongora, C. Moran, A. Iriarte, J. McCormack, S. C. Burgess, S. V. Edwards, E. Lyons, C. Williams, M. Breen, J. T. Howard, C. R. Gresham, D. G. Peterson, J. Schmitz, D. D. Pollock, D. Haussler, E. W. Triplett, G. Zhang, N. Irie, E. D. Jarvis, C. A. Brochu, C. J. Schmidt, F. M. McCarthy, B. C. Faircloth, F. G. Hoffmann, T. C. Glenn, T. Gabaldón, B. Paten, and D. A. Ray. 2014. Three crocodilian genomes reveal ancestral patterns of evolution among archosaurs. Science 346:1254449. doi: 10.1126/science.1254449.

Griffen, B. D., and H. Mosblack. 2011. Predicting diet and consumption rate differences between and within species using gut ecomorphology. Journal of Animal Ecology 80:854–863.

Harvey, P. H., and M. D. Pagel. 1991. The comparative method in evolutionary biology. Oxford University Press, New York, New York.

Healy, K., L. McNally, G. D. Ruxton, N. Cooper, and A. L. Jackson. 2013. Metabolic rate and body size are linked with perception of temporal information. Animal Behaviour 86:685–696.

Hilderbrand, G. V., S. D. Farley, C. T. Robbins, T. A. Hanley, K. Titus, and C. Servheen. 1996. Use of stable isotopes to determine diets of living and extinct bears. Canadian Journal of Zoology 74:2080-2088.

Hone, D. W. E., and M. J. Benton. 2005. The evolution of large size: how does Cope's Rule work? Trends in Ecology and Evolution 20:4–6.

Hotton III, N., E. C. Olson, and R. Beerbower. 1997. Chapter 7 - Amniote Origins and the Discovery of Herbivory; pp. 207–264 in S. S. Sumida and K. L. M. Martin (eds.), Amniote Origins. Academic Press, San Diego, California.

Hurlburt, G. 1999. Comparison of body mass estimation techniques, using recent reptiles and the pelycosaur *Edaphosaurus boanerges*. Journal of Vertebrate Paleontology 19:338–350.

Janis, C. M., and M. Carrano. 1992. Scaling of reproductive turnover in archosaurs and mammals: why are large terrestrial mammals so rare? Annales Zoologici Fennici 28:201–216.

Jones, K. E., S. Gonzalez, K. D. Angielczyk, and S. E. Pierce. 2020. Regionalization of the axial skeleton predates functional adaptation in the forerunners of mammals. Nature Ecology and Evolution 4:470–478.

Kissling, W. D., L. Dalby, C. Fløjgaard, J. Lenoir, B. Sandel, C. Sandom, K. Trøjelsgaard, and J.-C. Svenning. 2014. Establishing macroecological trait datasets: digitalization,

extrapolation, and validation of diet preferences in terrestrial mammals worldwide. Ecology and Evolution 4:2913–2930.

Kram, R., and C. R. Taylor. 1990. Energetics of running: a new perspective. Nature 346:265–267.

Law, C. J. 2019. Evolutionary shifts in extant mustelid (Mustelidae: Carnivora) cranial shape, body size and body shape coincide with the Mid-Miocene Climate Transition. Biology Letters 15:20190155. doi: 10.1098/rsbl.2019.0155.

Lehman, T. M. 1998. A gigantic skull and skeleton of the horned dinosaur *Pentaceratops sternbergi* from New Mexico. Journal of Paleontology 72:894–906.

Losos, J. B., and H. W. Greene. 1988. Ecological and evolutionary implications of diet in monitor lizards. Biological Journal of the Linnean Society 35:379–407.

Mallison, H. 2010. The digital *Plateosaurus* I: body mass, mass distribution and posture assessed using CAD and CAE on a digitally mounted complete skeleton. Palaeontoligica Electronica 13:1–27.

Marutho, D., S. H. Handaka, E. Wijaya, and Muljono. 2018. The determination of cluster number at k-mean using elbow method and purity evaluation on headline news. 2018 International Seminar on Application for Technology of Information and Communication 533–538.

O'Grady, S. P., M. Morando, L. Avila, and M. D. Dearing. 2005. Correlating diet and digestive tract specialization: examples from the lizard family Liolaemidae. Zoology 108:201–210.

Olden, J., Z. Hogan, and J. Vander Zanden. 2007. Small fish, big fish, red fish, blue fish: size-biased extinction risk of the world's freshwater and marine fishes. Global Ecology and Biogeography 16:694–701.

Oonincx, D. G. A. B., J. P. van Leeuwen, W. H. Hendriks, and A. F. B. van der Poel. 2015. The diet of free-roaming Australian Central Bearded Dragons (*Pogona vitticeps*). Zoo Biology 34:271–277.

Pianka, E. R., and R. B. Huey. 1978. Comparative ecology, resource utilization and niche segregation among gekkonid lizards in the southern Kalahari. Copeia 1978:691–701.

Pineda-Munoz, S., and J. Alroy. 2014. Dietary characterization of terrestrial mammals. Proceedings of the Royal Society B: Biological Sciences 281:20141173.

Porter, W. P., and M. Kearney. 2009. Size, shape, and the thermal niche of endotherms. Proceedings of the National Academy of Sciences 106:19666–19672.

Pough, F. H. 1973. Lizard energetics and diet. Ecology 54:837–844.

Pyron, M. 1999. Relationships between geographical range size, body size, local abundance, and habitat breadth in North American suckers and sunfishes. Journal of Biogeography 26:549–558.

R Core Team (2021). R: A language and environment for statistical computing. R Foundation for Statistical Computing, Vienna, Austria. URL https://www.R-project.org/.

Russell, E. S. 1916. Form and Function: A Contribution to the History of Animal Morphology. J. Murray, London, 383 pp.

Schoch, C. L., S. Ciufo, M. Domrachev, C. L. Hotton, S. Kannan, R. Khovanskaya, D. Leipe, R. Mcveigh, K. O'Neill, B. Robbertse, S. Sharma, V. Soussov, J. P. Sullivan, L. Sun, S. Turner, and I. Karsch-Mizrachi. 2020. NCBI Taxonomy: a comprehensive update on curation, resources and tools. Database: The Journal of Biological Databases and Curation 2020.

Seebacher, F. 2001. A new method to calculate allometric length-mass relationships of dinosaurs. Journal of Vertebrate Paleontology 21:51–60.

Sellers, W. I., J. Hepworth-Bell, P. L. Falkingham, K. T. Bates, C. A. Brassey, V. M. Egerton, and P. L. Manning. 2012. Minimum convex hull mass estimations of complete mounted skeletons. Biology Letters 8:842–845.

Simões, T. R., M. W. Caldwell, M. Tałanda, M. Bernardi, A. Palci, O. Vernygora, F. Bernardini, L. Mancini, and R. L. Nydam. 2018. The origin of squamates revealed by a Middle Triassic lizard from the Italian Alps. Nature 557:706–709.

Sommerfeldt, D., and C. Rubin. 2001. Biology of bone and how it orchestrates the form and function of the skeleton. European Spine Journal 10:S86–S95.

Springer, M. S., M. J. Stanhope, O. Madsen, and W. W. de Jong. 2004. Molecules consolidate the placental mammal tree. Trends in Ecology and Evolution 19:430–438.

Stevens, C. E., and I. D. Hume. 1998. Contributions of microbes in vertebrate gastrointestinal tract to production and conservation of nutrients. Physiological Reviews 78:393–427.

St-Pierre, B., and A.-D. G. Wright. 2012. Molecular analysis of methanogenic archaea in the forestomach of the alpaca (*Vicugna pacos*). BMC Microbiology 12:1. doi: 10.1186/1471-2180-12-1.

Sues, H.-D., and R. R. Reisz. 1998. Origins and early evolution of herbivory in tetrapods. Trends in Ecology and Evolution 13:141–145.

Swihart, R., N. A. Slade, and B. J. Bergstrom. 1988. Relating body size to the rate of home range use in mammals. Ecology 69:393–399.

Thompson, D. W. 1917. On Growth and Form. Cambridge University Press, Cambridge, United Kingdom. 793 pp.

Treves, F. 1886. Abstracts of six lectures on the intestinal canal and peritoneum in the Mammalia. British Medical Journal 1:583–584.

Troyer, K. 1984. Diet selection and digestion in *Iguana iguana*: the importance of age and nutrient requirements. Oecologia 61:201–207.

Upham, N. S., J. A. Esselstyn, and W. Jetz. 2019. Inferring the mammal tree: species-level sets of phylogenies for questions in ecology, evolution, and conservation. PLoS Biology 17:e3000494. doi: 10.1371/journal.pbio.3000494.

Vanover, A. 2014. Volume, lateral area, and surface area of an elliptic conical frustum. Mathematics Stack Exchange. Available at https://math.stackexchange.com/questions/973875/volume-lateral-area-and-surface-area-of-an-elliptic-conical-frustum. Accessed February 18, 2020.

Vermeij, G. J. 1994. The evolutionary interaction among species: selection, escalation, and coevolution. Annual Review of Ecology and Systematics 25:219–236.

Wagner, C. E., P. B. McIntyre, K. S. Buels, D. M. Gilbert, and E. Michel. 2009. Diet predicts intestine length in Lake Tanganyika's cichlid fishes. Functional Ecology 23:1122–1131.

Wang, D., Y. Pei, J. Yang, and Z. Wang. 2003. Digestive tract morphology and food habits in six species of rodents. Folia Zoologica 52:51–55.

Werner, J., and E. M. Griebeler. 2011. Reproductive biology and its impact on body size: comparative analysis of mammalian, avian and dinosaurian reproduction. PLoS ONE 6:e28442. doi: 10.1371/journal.pone.0028442.

West, K., A. Cohen, and M. Baron. 1991. Morphology and behavior of crabs and gastropods from Lake Tanganyika, Africa: implications for lacustrine predator-prey coevolution. Evolution 45:589–607.

Woronowicz, K. C., and R. A. Schneider. 2019. Molecular and cellular mechanisms underlying the evolution of form and function in the amniote jaw. EvoDevo 10:17. doi: 10.1186/s13227-019-0131-8.

Zaiontz, C. (2021) Real Statistics Resource Pack | Real Statistics Using Excel. Available at https://www.real-statistics.com/free-download/real-statistics-resource-pack/. Accessed June 23, 2021.

Ziegler, T., M. Strauch, T. Pes, J. Konas, T. Jirasek, N. Rütz, J. Oberreuter, and S. Holst. 2009. First captive breeding of the blue tree monitor *Varanus macraei*. Böhme & Jacobs, 2001 at the Plzen and Cologne Zoos. Biawak 3:122-133.

Table 1. Summary of cluster means for the 10 torso shape groups determined by *k*-means clustering using the eight torso shape variables that had been log-transformed and size-corrected with TTL as the denominator.

Shape	ATL	PTL	MTH	MTW	ATH	ATW	PTH	PTW
1	0.8344911	0.8568975	0.6192353	0.7735068	0.3382179	0.3916277	0.4274921	0.4615036
2	0.7891339	0.8873817	0.6976236	0.2479480	0.5196751	0.4043858	0.5788886	0.3128756
3	0.8618847	0.9021933	0.8359473	0.8416129	0.6741644	0.6704513	0.7742935	0.7596914
4	0.8306726	0.8972554	0.7938519	0.8081783	0.5155719	0.6016782	0.7005440	0.6957560
5	0.8945100	0.8915042	0.8821560	0.8962765	0.7649674	0.7149196	0.8212604	0.8003460
6	0.7765947	0.9367320	0.7913745	0.7489380	0.6256196	0.6004508	0.2525615	0.6674446
7	0.8492507	0.9031309	0.8109587	0.7892713	0.6462951	0.5748690	0.6946731	0.7022087
8	0.8707533	0.8556111	0.6324954	0.8093228	0.5560233	0.6302704	0.6178679	0.6648955
9	0.7935380	0.8811547	0.6864392	0.6551403	0.4563104	0.5102914	0.5475432	0.6282442
10	0.8755585	0.8776027	0.7492727	0.8523520	0.6821267	0.7322081	0.6899418	0.7233567

Table 2. Summary of cluster (interpreted as torso shape group) assignments following *k*-means clustering. Table includes: Species Code (SC), scientific name, common name, diet classification, and taxonomic rank.

SC	Species	Common name	Diet	Class	Order
TORSO SHAPE GROUP 1 (*n* = 4)					
17	*Varanus macraei*	Blue tree monitor	C	R	Squamata
66	*Scapanus latimanus*	Broad-footed mole	C	M	Eulipotyphyla
67	*Blarina brevicauda*	Northern short-tailed shrew	C	M	Eulipotyphyla
88	*Mustela vison*	American mink	C	M	Carnivora
TORSO SHAPE GROUP 2 (*n* = 1)					
20	*Bradypodion fischeri*	Fischer's chameleon	C	R	Squamata
TORSO SHAPE GROUP 3 (*n* = 22)					
26	*Tachyglossus aculeatus*	Short-nosed echidna	C	M	Monotremata
27	*Macropus parryi*	Pretty-faced wallaby	H	M	Diprotodontia
30	*Sarcophilus harrisii*	Tasmanian devil	C	M	Dasyuromorphia
34	*Orycteropus afer*	Aardvark	C	M	Tubulidentata
36	*Procavia capensis*	Rock hyrax	H	M	Hyracoidea
39	*Dasypus novemcinctus*	Nine-banded armadillo	C	M	Cingulata
40	*Choloepus hoffmanni*	Two-toed sloth	H	M	Pilosa
48	*Mandrillus sphinx*	Mandrill	H	M	Primates
56	*Hydrochoerus hydrochaeris*	Capybara	H	M	Rodentia
62	*Erethizon dorsatum*	North American porcupine	H	M	Rodentia
70	*Canis lupus*	Wolf	C	M	Carnivora
80	*Panthera leo*	Lion	C	M	Carnivora
91	*Nasua nasua*	South American coati	O	M	Carnivora
95	*Proteles cristatus*	Aardwolf	C	M	Carnivora
98	*Tremarctos ornatus*	Spectacled bear	H	M	Carnivora
99	*Ursus americanus*	American black bear	H	M	Carnivora
101	*Arctictis binturong*	Binturong	O	M	Carnivora
104	*Manis pentadactyla*	Chinese pangolin	C	M	Pholidota
108	*Ammotragus lervia*	Barbary sheep	H	M	Artiodactyla
110	*Cephalophus silvicultor*	Yellow-backed duiker	H	M	Artiodactyla

114	*Vicugna pacos*	Alpaca	H	M	Artiodactyla
116	*Odocoileus virginianus*	White-tailed deer	H	M	Artiodactyla

TORSO SHAPE GROUP 4 (*n* = 26)

31	*Didelphis virginiana*	Virginia opossum	O	M	Didelphimorphia
32	*Tenrec ecaudatus*	Common tenrec	C	M	Afrosoricida
33	*Rhynchocyon petersi*	Zanj elephant shrew	C	M	Macroscelidea
37	*Chaetophractus villosus*	Big hairy armadillo	O	M	Cingulata
42	*Galeopterus variegatus*	Malayan colugo	H	M	Dermoptera
45	*Varecia variegata*	Black-and-white ruffed lemur	H	M	Primates
46	*Cercopithecus diana*	Diana monkey	O	M	Primates
47	*Macaca mulatta*	Rhesus macaque	H	M	Primates
51	*Oryctolagus cuniculus*	European rabbit	H	M	Lagomorpha
52	*Ochotona collaris*	Collared pika	H	M	Lagomorpha
53	*Aplodontia rufa rufa*	Mountain beaver	H	M	Rodentia
54	*Bathyergus suillus*	Cape dune mole-rat	H	M	Rodentia
55	*Castor canadensis*	North American beaver	H	M	Rodentia
57	*Neofiber alleni alleni*	Round-tailed muskrat	H	M	Rodentia
58	*Ondatra zibethicus*	Muskrat	H	M	Rodentia
63	*Cricetomys gambianus*	Gambian pouched rat	O	M	Rodentia
64	*Pedetes capensis*	Springhare	H	M	Rodentia
65	*Erinaceus europaeus*	European hedgehog	C	M	Eulipotyphyla
73	*Vulpes zerda*	Fennec fox	C	M	Carnivora
77	*Felis catus*	Domestic cat	C	M	Carnivora
82	*Mephitis macroura*	Hooded skunk	O	M	Carnivora
84	*Enhydra lutris*	Sea otter	C	M	Carnivora
85	*Lontra canadensis*	Common otter	C	M	Carnivora
86	*Martes pennanti*	Fisher	C	M	Carnivora
90	*Nasua narica narica*	White-nosed coati	O	M	Carnivora
93	*Crossarchus platycephalus*	Flat-headed kusimanse	C	M	Carnivora

TORSO SHAPE GROUP 5 (*n* = 14)

16	*Varanus komodoensis*	Komodo dragon	C	R	Squamata
29	*Phascolarctos cinereus*	Koala	H	M	Diprotodontia
35	*Loxodonta africana*	African elephant	H	M	Proboscidea
38	*Euphractus sexcinctus*	Six-banded armadillo	O	M	Cingulata

41	*Myrmecophaga tridactyla*	Giant anteater	C	M	Pilosa
49	*Gorilla gorilla*	Western gorilla	H	M	Primates
100	*Ursus arctos horribilis*	Grizzly bear	O	M	Carnivora
105	*Equus ferus caballus*	Domestic horse	H	M	Perissodactyla
106	*Ceratotherium simum*	White rhinoceros	H	M	Perissodactyla
107	*Tapirus indicus*	Malayan tapir	H	M	Perissodactyla
109	*Bison bison*	American bison	H	M	Artiodactyla
117	*Giraffa camelopardalis*	Giraffe	H	M	Artiodactyla
118	*Hippopotamus amphibious*	Hippopotamus	H	M	Artiodactyla
119	*Babyrousa celebensis*	Sulawesi babirusa	H	M	Artiodactyla
TORSO SHAPE GROUP 6 (*n* = 1)					
44	*Eulemur macaco*	Black lemur	H	M	Primates
TORSO SHAPE GROUP 7 (*n* = 27)					
50	*Brachylagus idahoensis*	Pygmy rabbit	H	M	Lagomorpha
59	*Cuniculus paca*	Lowland paca	H	M	Rodentia
60	Dasyprocta (sp. indet.)	Agouti	H	M	Rodentia
68	*Canis aureus*	Golden jackal	C	M	Carnivora
69	*Canis latrans*	Coyote	C	M	Carnivora
71	*Cerdocyon thous*	Crab-eating fox	C	M	Carnivora
72	*Speothos venaticus*	Bush dog	C	M	Carnivora
74	*Vulpes lagopus lagopus*	Arctic fox	C	M	Carnivora
75	*Vulpes vulpes*	Red fox	C	M	Carnivora
76	*Cryptoprocta ferox*	Fossa	C	M	Carnivora
78	*Lynx rufus*	Bobcat	C	M	Carnivora
79	*Neofelis nebulosa*	Clouded leopard	C	M	Carnivora
81	*Conepatus leuconotus*	Hog-nosed skunk	C	M	Carnivora
83	*Mephitis mephitis*	Striped skunk	O	M	Carnivora
89	*Gulo gulo luscus*	Wolverine	C	M	Carnivora
92	*Potos flavus*	Kinkajou	H	M	Carnivora
94	*Mungos mungo*	Banded mongoose	C	M	Carnivora
102	*Genetta genetta*	Common genet	C	M	Carnivora
111	*Gazella dorcas*	Dorcas gazelle	H	M	Artiodactyla
112	*Gazella spekei*	Speke's gazelle	H	M	Artiodactyla
113	*Philantomba monticola*	Blue duiker	H	M	Artiodactyla
115	*Muntiacus reevesi*	Reeve's muntjac	H	M	Artiodactyla
120	*Sus scrofa domesticus*	Domestic pig	H	M	Artiodactyla
121	*Pecari tajacu*	Collared peccary	H	M	Artiodactyla
122	Tayassuidae (sp. indet.)	Peccary	H	M	Artiodactyla

123	*Moschiola memmina*	Spotted mouse-deer	H	M	Artiodactyla
124	*Tragulus napu borneanus*	Greater mouse-deer	H	M	Artiodactyla
TORSO SHAPE GROUP 8 (*n* = 10)					
2	*Alligator mississpiensis*	American alligator	C	R	Crocodilia
5	*Paleosuchus palpebrosus*	Cuvier's dwarf caiman	C	R	Crocodilia
10	*Trachydosaurus rugosus*	Shingleback lizard	H	R	Squamata
11	*Tiliqua scincoides*	Blue-tongued lizard	H	R	Squamata
13	*Heloderma horridum*	Beaded lizard	C	R	Squamata
14	*Heloderma suspectum*	Gila monster	C	R	Squamata
15	*Varanus griseus*	Desert monitor	C	R	Squamata
18	*Varanus rudicollus*	Rough-neck monitor	C	R	Squamata
21	*Uromastyx aegyptius*	Egyptian mastigure	H	R	Squamata
23	*Dipsosaurus dorsalis*	Desert iguana	H	R	Squamata
TORSO SHAPE GROUP 9 (*n* = 6)					
9	*Chondrodactylus bibronii*	Bibron's gecko	C	R	Squamata
28	*Petaurus breviceps*	Sugar glider	O	M	Diprotodontia
43	*Tupaia javanica*	Javan treeshrew	C	M	Scandentia
61	*Heterocephalus glaber*	Naked mole-rat	H	M	Rodentia
87	*Mustela erminea*	Ermine	C	M	Carnivora
103	*Paradoxurus hermaphroditus*	Asian palm civet	O	M	Carnivora
TORSO SHAPE GROUP 10 (*n* = 13)					
1	*Alligator sinensis*	Chinese alligator	C	R	Crocodilia
3	*Caiman crocodilus yacare*	Yacare caiman	C	R	Crocodilia
4	*Caiman crocodilus*	Spectacled caiman	C	R	Crocodilia
6	*Crocodylus porosus*	Saltwater crocodile	C	R	Crocodilia
7	*Gavialis gangeticus*	Gharial	C	R	Crocodilia
8	*Sphenodon punctatus*	Tuatara	C	R	Rhynchocephalia
12	*Salvator merianae*	Black and white tegu	O	R	Squamata
19	*Varanus salvator*	Water monitor	C	R	Squamata
22	*Pogona vitticeps*	Bearded dragon	O	R	Squamata
24	*Iguana iguana*	Green iguana	H	R	Squamata
25	*Ornithorhynchus anatinus*	Platypus	C	M	Monotremata
96	*Zalophus californianus*	California sea lion	C	M	Carnivora
97	*Monachus schauinslandi*	Hawaiian monk seal	C	M	Carnivora

Table 3. Mean standardized and size-corrected MHL and MFL values and standard error for original 10 torso shape groups determined by *k*-means clustering.

Torso Shape Group	*Count*	*Mean MHL (Std Err)*	*Mean MFL (Std Err)*
Shape 1	4	0.6491 (0.0344)	0.6553 (0.0305)
Shape 2	1	0.6645 (N/A)	0.6761 (N/A)
Shape 3	22	0.8267 (0.0092	0.8505 (0.0068)
Shape 4	26	0.7762 (0.0084)	0.8124 (0.0093)
Shape 5	14	0.8347 (0.0117)	0.8617 (0.0100)
Shape 6	1	0.8136 (N/A)	0.8706 (N/A)
Shape 7	27	0.8001 (0.0046)	0.8272 (0.0040)
Shape 8	10	0.6840 (0.0188)	0.7019 (0.0231)
Shape 9	6	0.7155 (0.0360)	0.7336 (0.0277)
Shape 10	13	0.7476 (0.0071)	0.7577 (0.0128)

Table 4. Mean standardized and size-corrected MHL and MFL values and standard error for consolidated seven torso shape groups (Shape 2 removed) determined by *k*-means clustering.

Torso Shape Group	*Count*	*Mean MHL (Std Err)*	*Mean MFL (Std Err)*
Shape 1+10	17	0.7244 (0.0138)	0.7336 (0.0156)
Shape 3	22	0.8267 (0.0092)	0.8505 (0.0067)
Shape 4	26	0.7762 (0.0084)	0.8124 (0.0093)
Shape 5	14	0.8347 (0.0116)	0.8617 (0.0999)
Shape 6 + 7	28	0.8005 (0.0044)	0.8287 (0.0041)
Shape 8	10	0.6840 (0.0188)	0.7019 (0.0230)
Shape 9	6	0.7155 (0.0360)	0.7336 (0.0277)

Table 5. Results of Dunn's test following Kruskal-Wallis for mean log-transformed and size-corrected MHL by original 10 torso shape groups.

Torso Shape Group	Median	*z*-statistics (*p*-values indicated in parentheses)									
		1	2	3	4	5	6	7	8	9	10
1. Torso Shape 1	0.667	-									
2. Torso Shape 2	0.664	0.024	-								
3. Torso Shape 3	0.820	4.241**	2.282* (0.02)	-							
4. Torso Shape 4	0.771	2.512* (0.01)	0.135	3.300**	-						
5. Torso Shape 5	0.830	4.287**	2.375* (0.01)	0.365	3.261**	-					
6. Torso Shape 6	0.813	1.990* (0.04)	1.593	0.077	0.860	0.197	-				
7. Torso Shape 7	0.800	3.460**	1.847	1.572	1.835	1.751	0.365	-			
8. Torso Shape 8	0.698	0.338	0.217	5.520**	3.088* (0.002)	5.386**	1.931	4.466**	-		
9. Torso Shape 9	0.738	1.185	0.734	3.344**	1.290	3.413**	1.352	2.412**	1.093	-	
10. Torso Shape 10	0.755	1.257	0.719	4.535**	1.855	4.443**	1.451	3.361**	1.233	0.093	-

* indicates significant differences ($p < 0.05$)
**indicates $p < 0.001$

Table 6. Results of Dunn's test following Kruskal-Wallis for mean log-transformed and size-corrected MHL by eight consolidated torso shape groups.

Torso Shape Group	Median	*z*-statistics (*p*-values indicated in parentheses)							
		1	2	3	4	5	6	7	8
1. Torso Shape 1+10	0.734	-							
2. Torso Shape 2	0.664	0.561	-						
3. Torso Shape 3	0.820	5.436**	2.282* (0.02)	-					
4. Torso Shape 4	0.771	2.563* (0.01)	1.351	3.300**	-				
5. Torso Shape 5	0.830	5.211**	2.375* (0.01)	0.365	3.261**	-			
6. Torso Shape 6+7	0.804	4.284**	1.862	1.538	1.900	1.721	-		
7. Torso Shape 8	0.698	0.877	0.217	5.520**	3.088**	5.386**	4.524**	-	
8. Torso Shape 9	0.738	0.454	0.734	3.344**	1.290	3.413**	2.449* (0.01)	1.093	-

*indicates significant differences ($p < 0.05$)
**indicates $p < 0.001$

Table 7. Results of Dunn's test following Kruskal-Wallis for mean log-transformed and size-corrected MHL by seven consolidated torso shape groups (torso shape 2 removed).

Torso Shape Group	Median	*z*-statistics (*p*-values indicated in parentheses)						
		1	2	3	4	5	6	7
1. Torso Shape 1+10	0.734	-						
2. Torso Shape 3	0.820	5.437**	-					
3. Torso Shape 4	0.771	2.573* (0.01)	3.327**	-				
4. Torso Shape 5	0.830	5.244**	0.368	3.361**	-			
5. Torso Shape 6+7	0.804	4.308**	1.55	1.916	1.735	-		
6. Torso Shape 8	0.698	0.871	5.542**	3.090* (0.002)	5.410**	4.538**	-	
7. Torso Shape 9	0.738	0.459	3.361**	1.290	3.431**	2.459* (0.01)	1.095	-

* indicates significant differences ($p < 0.05$)
**indicates $p < 0.001$

Table 8. Results of ANOVA for mean log-transformed and size-corrected MFL by original 10 torso shape groups.

Sources	*SS*	*df*	*MS*	*F*	*p*
Between Groups	0.38156939	9	0.0423966	22.5137091	1.5401E-21
Within Groups	0.21467863	114	0.00188315		
Total	0.59624802	123	0.00484754		

Table 9. Post hoc results for average MFL by original 10 torso shape groups.

Torso Shape Group	Mean	Mean Differences ($X_i – X_k$) (Effect Sizes are indicated in parentheses)									
		1	2	3	4	5	6	7	8	9	10
1. Torso Shape 1	0.655	-									
2. Torso Shape 2	0.676	0.021	-								
3. Torso Shape 3	0.851	0.195* (4.50)	0.174* (4.02)	-							
4. Torso Shape 4	0.812	0.157* (3.62)	0.136	0.038	-						
5. Torso Shape 5	0.862	0.206* (4.75)	0.186* (4.28)	0.011	0.049* (1.14)	-					
6. Torso Shape 6	0.871	0.215* (4.96)	0.195	0.020	0.058	0.009	-				
7. Torso Shape 7	0.827	0.172* (3.96)	0.151* (3.48)	0.023	0.015	0.035	0.043	-			
8. Torso Shape 8	0.702	0.047	0.026	0.149* (3.42)	0.110* (2.55)	0.160* (3.68)	0.169* (3.89)	0.125* (2.89)	-		
9. Torso Shape 9	0.734	0.078	0.058	0.117* (2.69)	0.079* (1.82)	0.128* (2.95)	0.137	0.094* (2.16)	0.032	-	
10. Torso Shape 10	0.758	0.102* (2.36)	0.082	0.093* (2.14)	0.055* (1.26)	0.104* (2.40)	0.113	0.069* (1.60)	0.056	0.024	-

*$p < 0.05$

Table 10. Results of ANOVA for mean log-transformed and size-corrected MFL by eight consolidated torso shape groups.

Sources	*SS*	*df*	*MS*	*F*	*P value*
Between Groups	0.34768694	7	0.04966956	23.1800943	2.0284E-19
Within Groups	0.24856108	116	0.00214277		
Total	0.59624802	123	0.00484754		

Table 11. Post Hoc Results for Average MFL by eight consolidated torso shape groups.

Torso Shape Group	Mean	Mean Differences ($X_i – X_k$) (Effect Sizes are indicated in parentheses)							
		1	2	3	4	5	6	7	8
1. Torso Shape 1+10	0.734	-							
2. Torso Shape 2	0.676	0.058	-						
3. Torso Shape 3	0.851	0.117* (2.52)	0.174* (3.77)	-					
4. Torso Shape 4	0.812	0.079* (1.70)	0.136	0.038	-				
5. Torso Shape 5	0.862	0.128* (2.76)	0.186* (4.01)	0.011	0.049* (1.07)	-			
6. Torso Shape 6+7	0.829	0.095	0.153* (3.30)	0.022	0.016	0.033	-		
7. Torso Shape 8	0.702	0.032	0.026	0.149* (3.21)	0.110* (2.39)	0.160* (3.45)	0.127* (2.74)	-	
8. Torso Shape 9	0.734	9.83E-06	0.058	0.117* (2.53)	0.079* (1.70)	0.128* (2.76)	0.095* (2.05)	0.032	-

*$p < 0.05$

Table 12. Results of ANOVA for mean log-transformed and size-corrected MFL by seven consolidated torso shape groups (torso shape 2 removed).

Sources	*SS*	*df*	*MS*	*F*	*P value*
Between Groups	0.33124497	6	0.0552075	25.7645701	2.7382E-19
Within Groups	0.24856108	116	0.00214277		
Total	0.57980605	122	0.00475251		

Table 13. Post hoc results for average MFL by seven consolidated torso shape groups (torso shape 2 removed).

Torso Shape Group	Mean	Mean Differences ($X_i – X_k$) (Effect Sizes are indicated in parentheses)						
		1	2	3	4	5	6	7
1. Torso Shape 1+10	0.734	-						
2. Torso Shape 3	0.851	0.117* (2.52)	-					
3. Torso Shape 4	0.812	0.079* (1.70)	0.038	-				
4. Torso Shape 5	0.862	0.128* (2.76)	0.011	0.049* (1.07)	-			
5. Torso Shape 6+7	0.829	0.095	0.022	0.016	0.033	-		
6. Torso Shape 8	0.702	0.032	0.149* (3.21)	0.110* (2.39)	0.160* (3.45)	0.127* (2.74)	-	
7. Torso Shape 9	0.734	9.83E-06	0.117* (2.53)	0.079* (1.70)	0.128* (2.76)	0.095* (2.05)	0.032	-

*$p < 0.05$

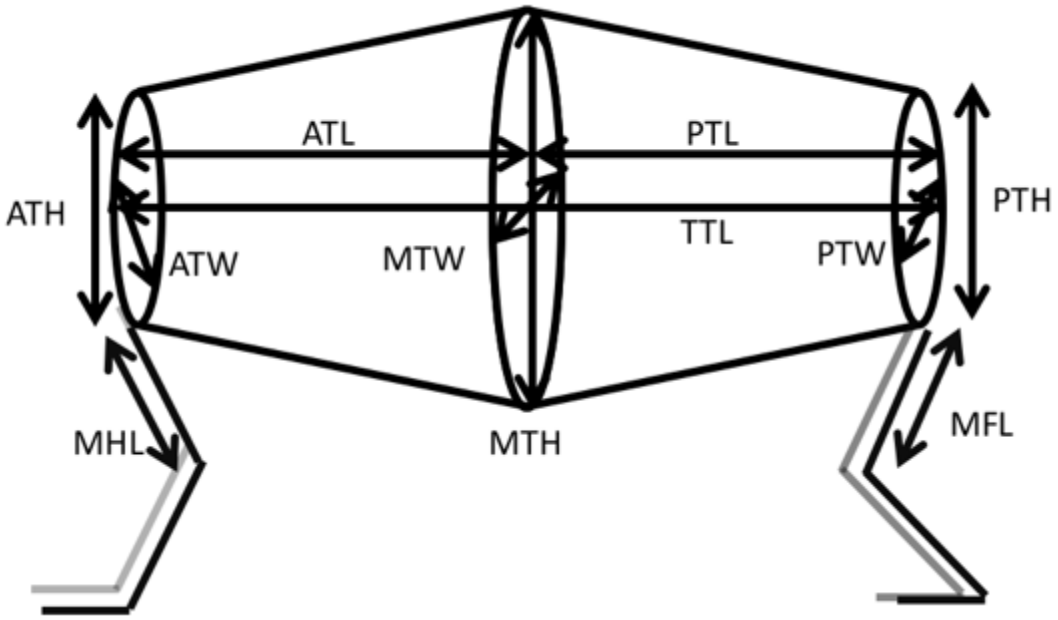

Figure 1. Schematic conceptual model for complex torso morphology. Torso variables include: total, anterior and posterior torso length (TTL, ATL, PTL), maximum torso width and height (MTW, MTH), anterior torso width and height (ATW, ATH), and posterior torso width and height (PTW, PTH). Limb variables include: maximum humerus length (MHL) and maximum femur length (MFL).

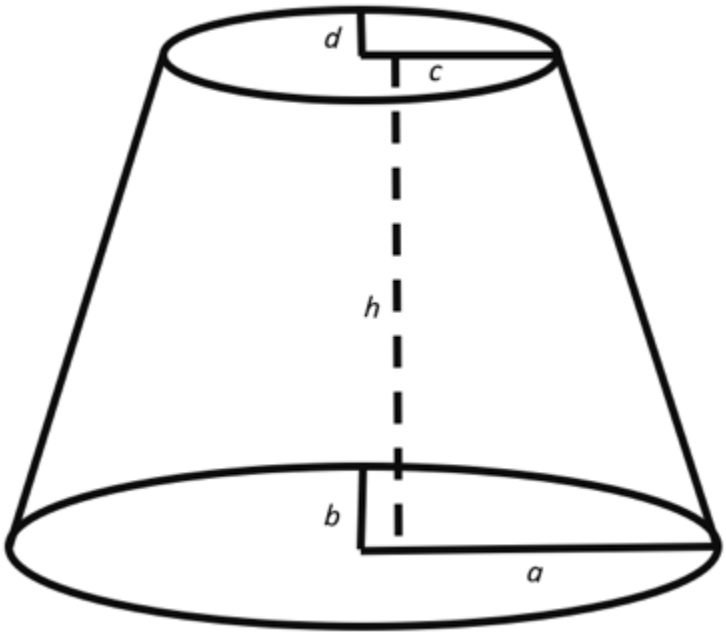

Figure 2. Elliptic conical frustum. In this figure, *a* represents the semi-major axis of the large base, *b* the semi-minor axis of the large base, *c* the semi-major axis of the small base, and *d* the semi-minor axis of the small base. The height of the frustum is represented by *h*.

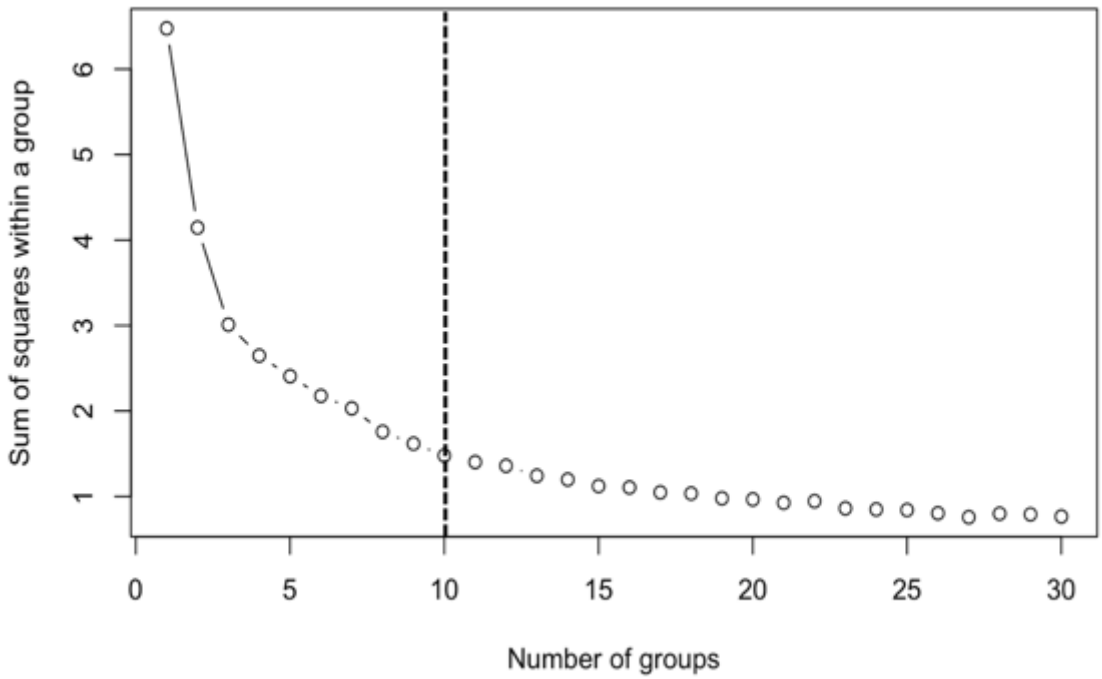

Figure 3. Elbow Curve from *k*-means clustering. Dotted line indicates the location where Sum of squares within a group begins to flatten out, suggesting that additional clusters would not impact the total WSS, thus the optimal number of groups is set at $k = 10$.

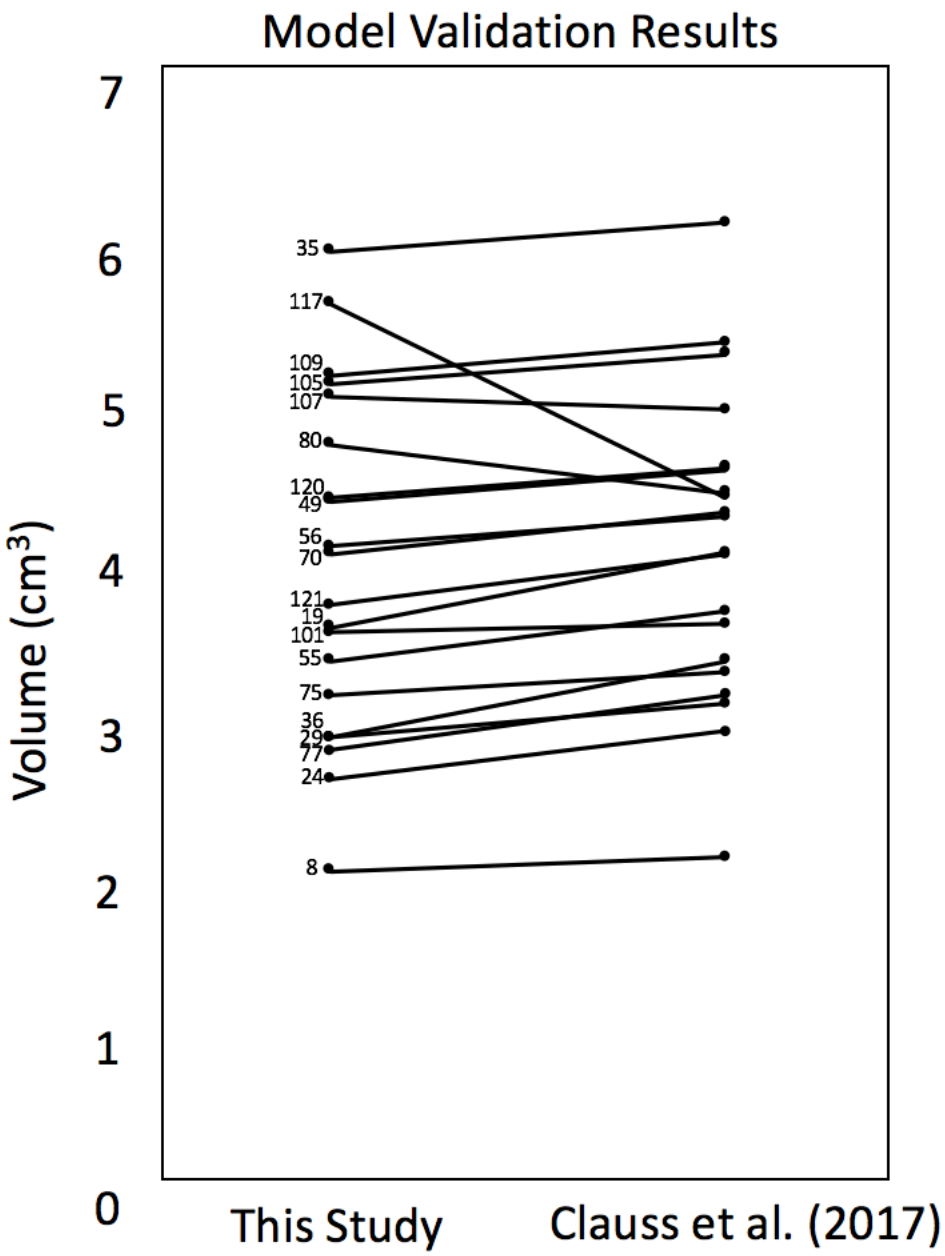

Figure 4. Graph depicting results from the paired *t*-test to determine the validity of the conceptual model (Fig. 1) when compared to the convex hull method used by Clauss et al. (2017) (numbers indicate species codes for the 20 amniotes in the *t*-test: see Appendix 2). The results of the *t*-test indicated that there was no significant difference in mean torso volumes calculated from the torso shape model ($\bar{x}$ = 4.03, *SD* = 1.07) and from those calculated using the digital convex hull method seen in that published study ($\bar{x}$ = 4.15, *SD* = 0.95), $t(19) = -1.56$, $p = 0.06$.

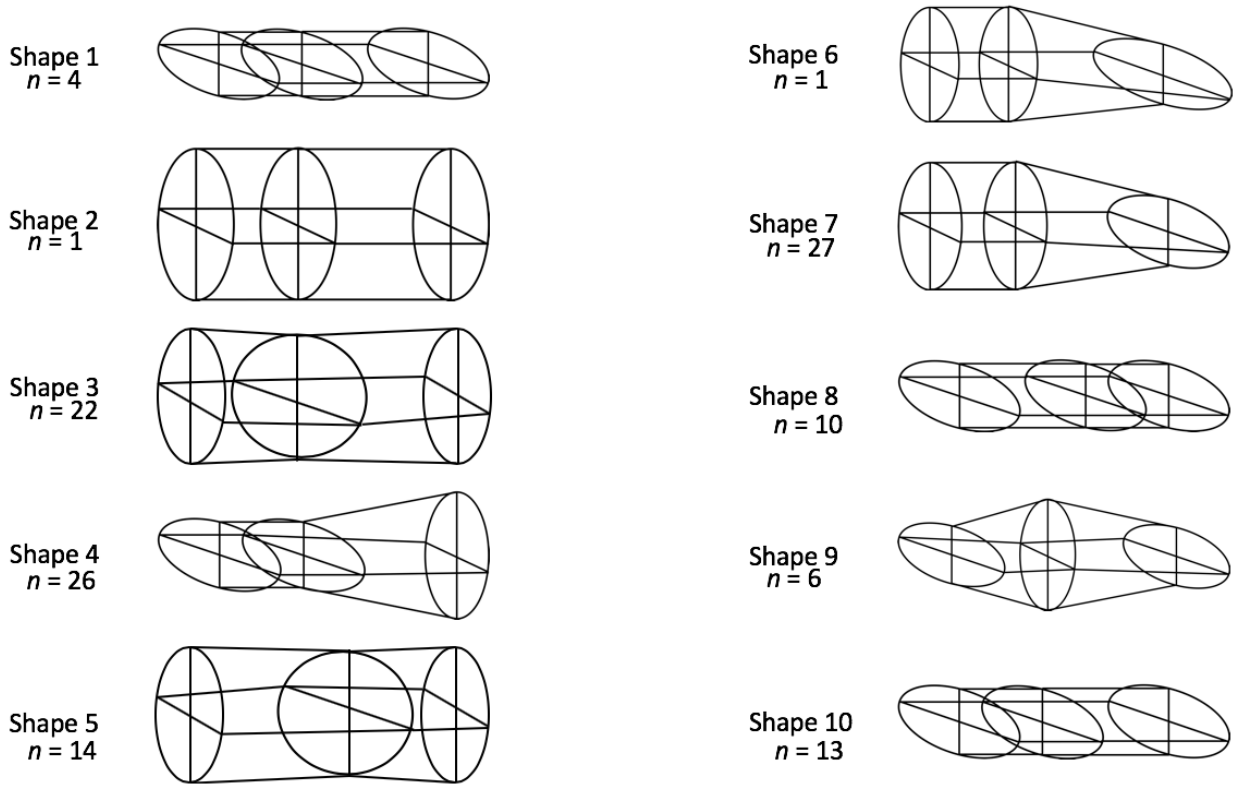

Figure 5. Conceptualized models and number of individuals (*n*) for the 10 torso shapes determined by *k*-means clustering. Ratios of average values of log-transformed and size-correct torso shape variables (Table 1) for each torso shape group were used to generate the models. Note that torso shapes 1 and 10 exhibit the same ratios of torso shape variables. Torso shapes 6 and 7 also have similar ratios, whereas torso shape 6 has a larger ratio of PTW to PTH. In both cases, these pairs were consolidated and individuals in these pairs of groups are considered to possess the same torso shape.

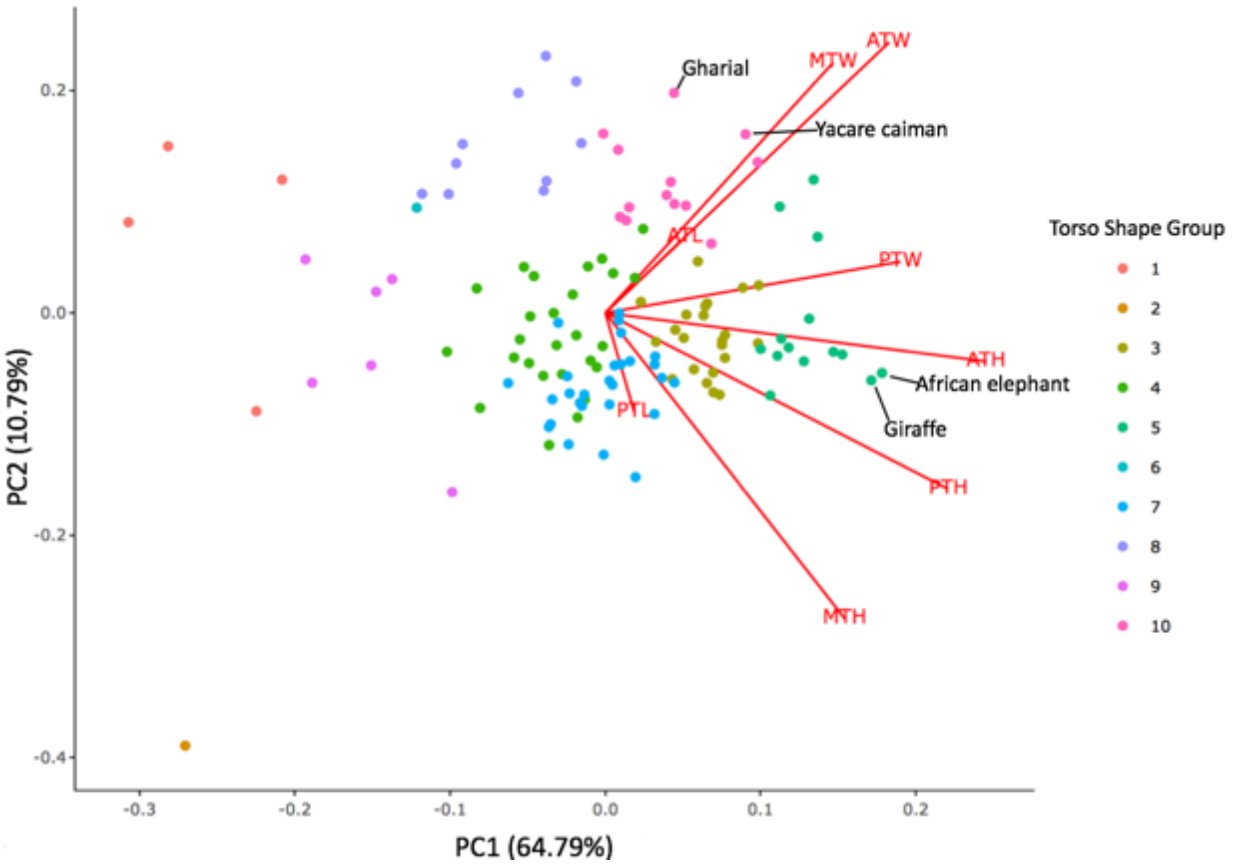

Figure 6. PCA scatter plot of the 10 original torso shape groupings. Percentage in parentheses on each axis denotes percent variation explained by that principal component. Loadings are represented by the red lines and labeled with torso shape variables.

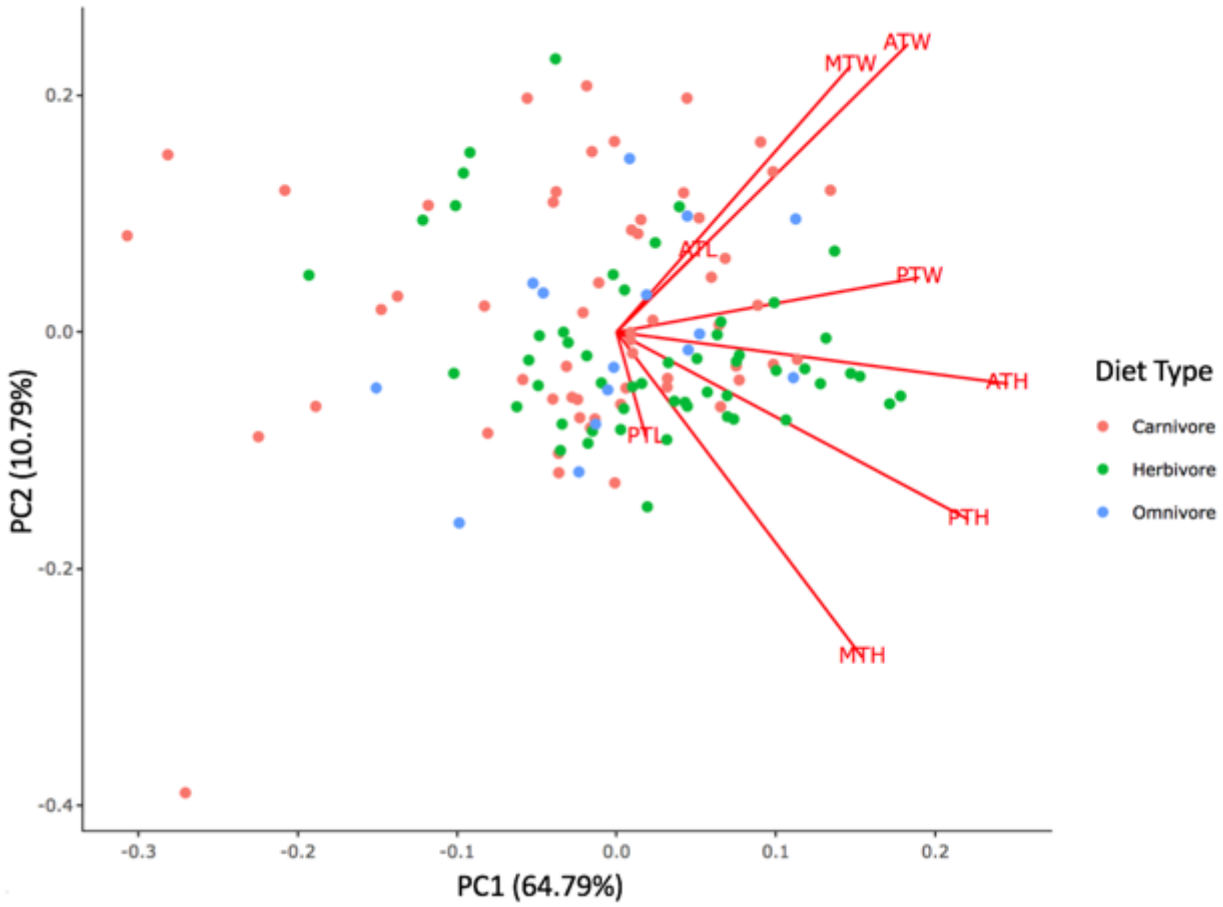

Figure 7. PCA scatter plot of amniote taxa coded for diet type. Percentage in parentheses on each axis denotes percent variation explained by that principal component. Loadings are represented by the red lines and labeled with torso shape variables.

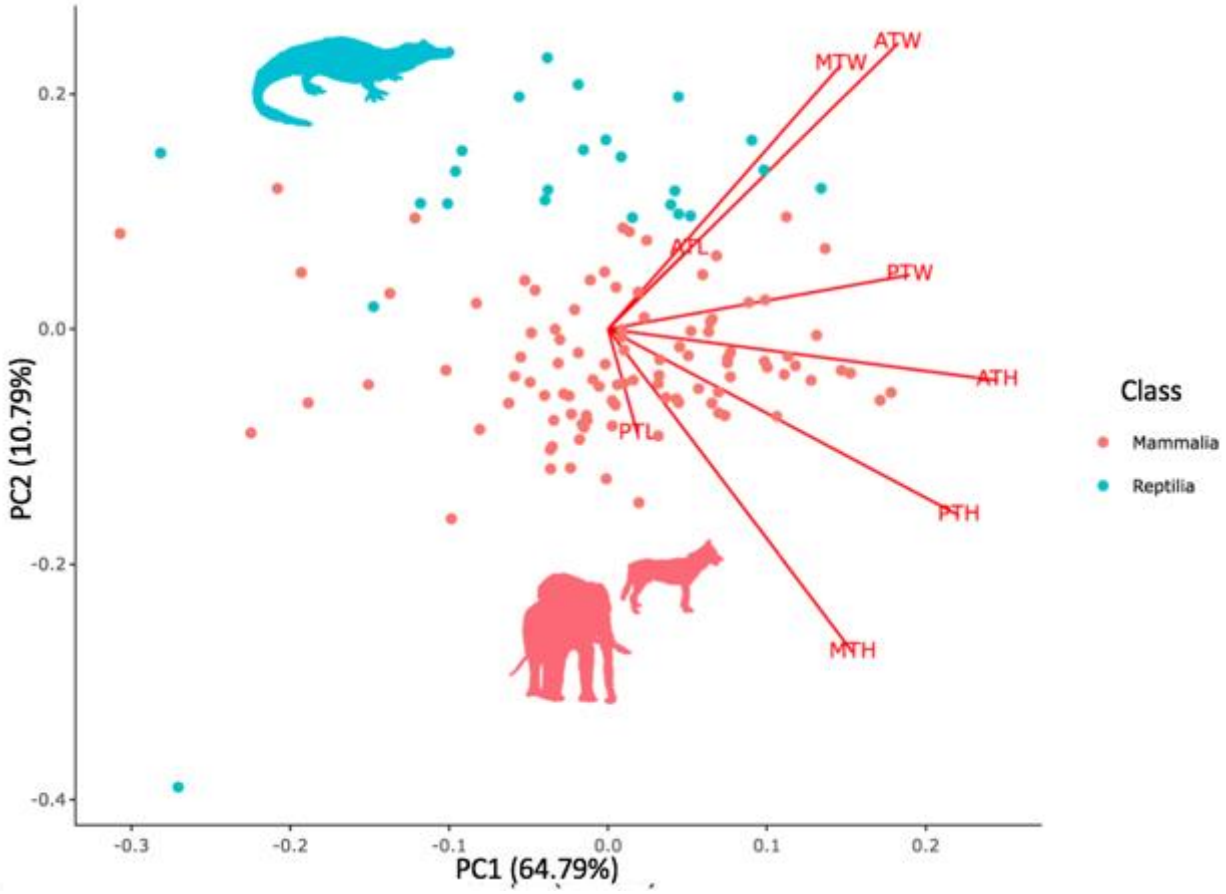

Figure 8. PCA scatter plot of amniote taxa coded for taxonomic class. Percentage in parentheses on each axis denotes percent variation explained by that principal component. Loadings are represented by the red lines and labeled with torso shape variables.

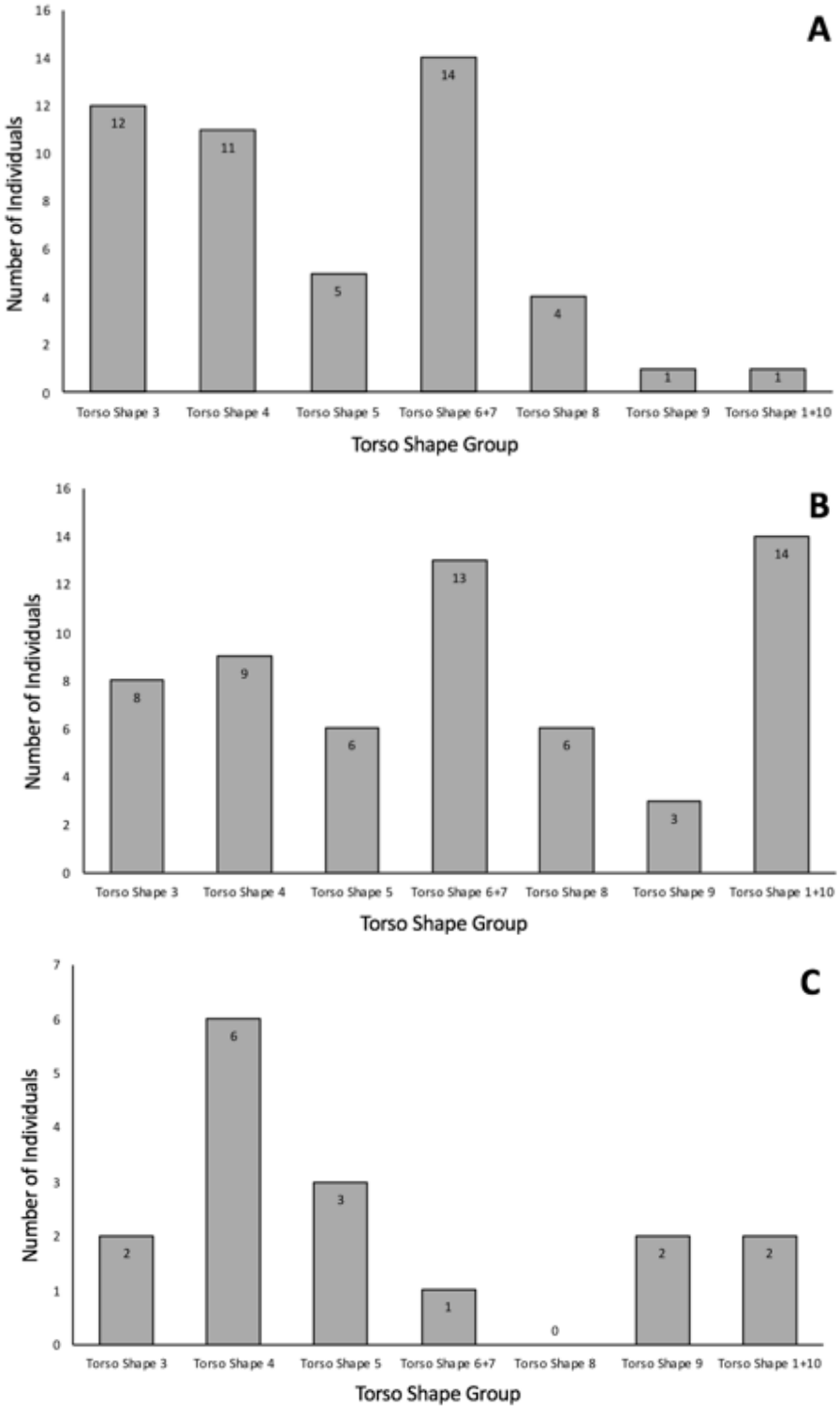

Figure 9. Distribution of torso shapes across diet types. Note that similar torso shapes were consolidated, and that torso shape 2 was removed. Also note the different scales for the different diets. Herbivores (A) and carnivores (B) were more abundant than omnivores (C) in this dataset.

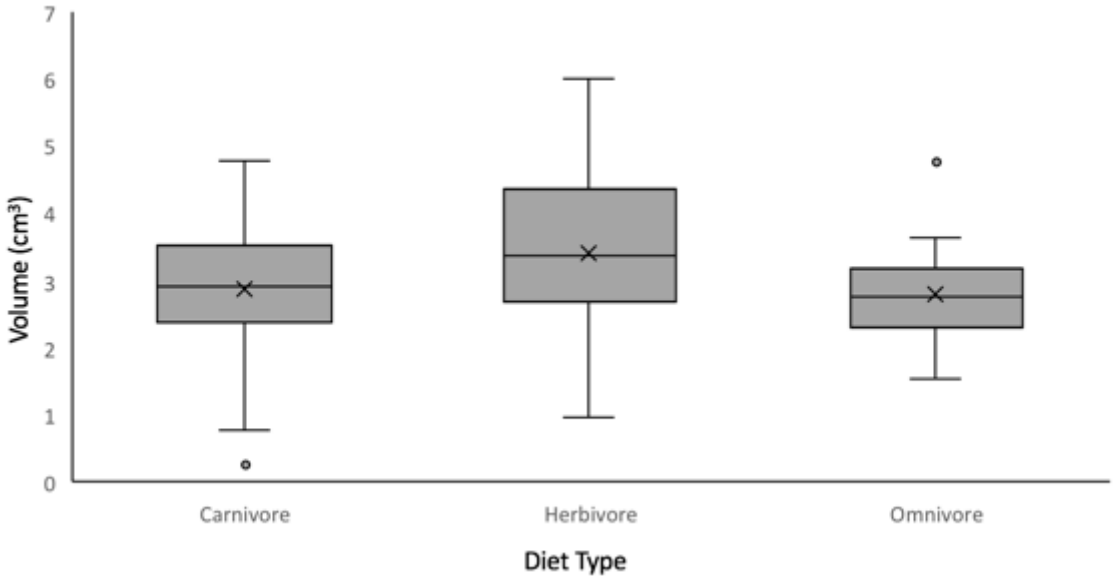

Figure 10. Average standardized and size-corrected volume for each of the three diet types.

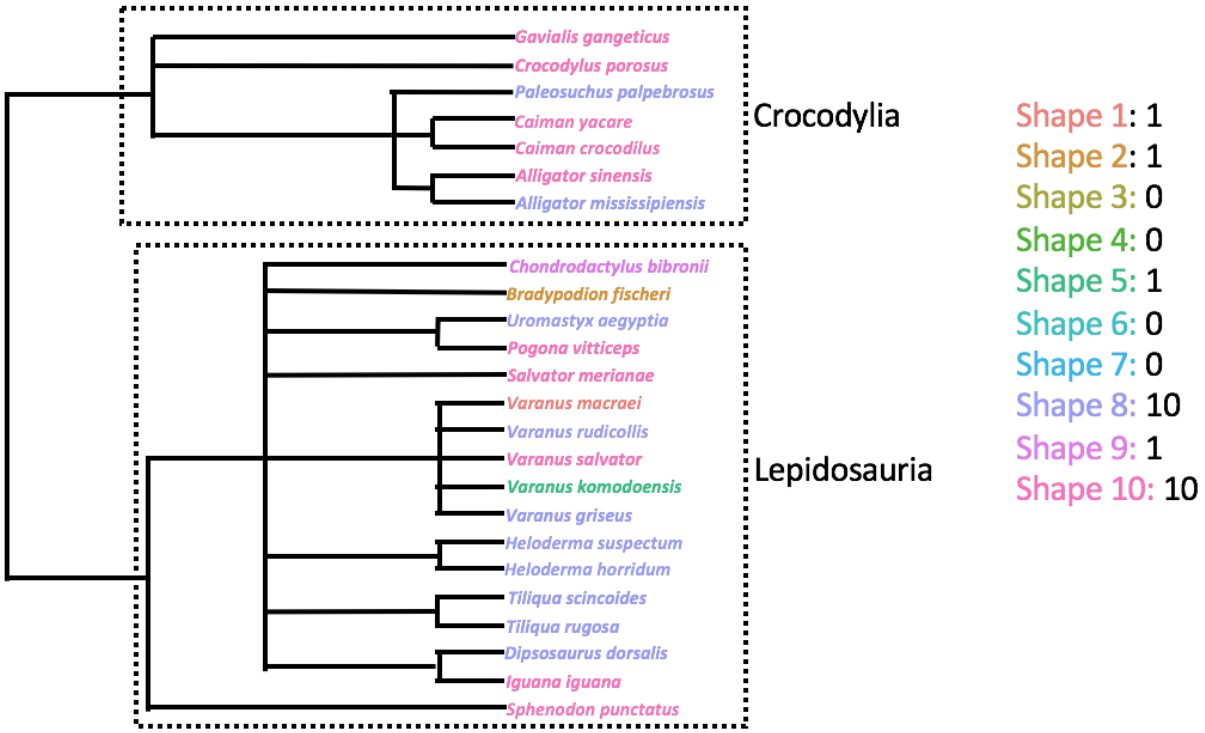

Figure 11. Representative phylogenetic tree of Reptilia from this study with torso shape group identified by color.

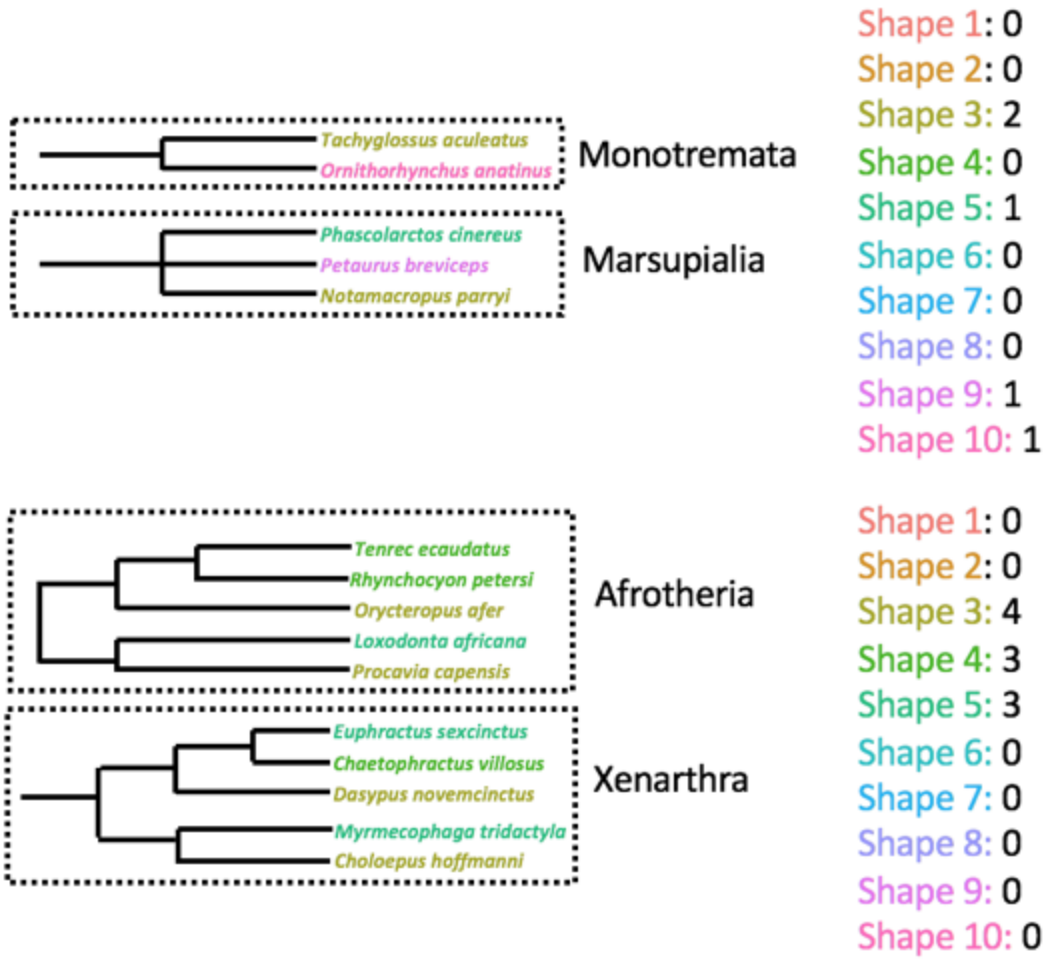

Figure 12. Representative phylogenetic trees of Monotremata and Marsupialia as well as Afrotheria and Xenarthra from this study with torso shape group identified by color.

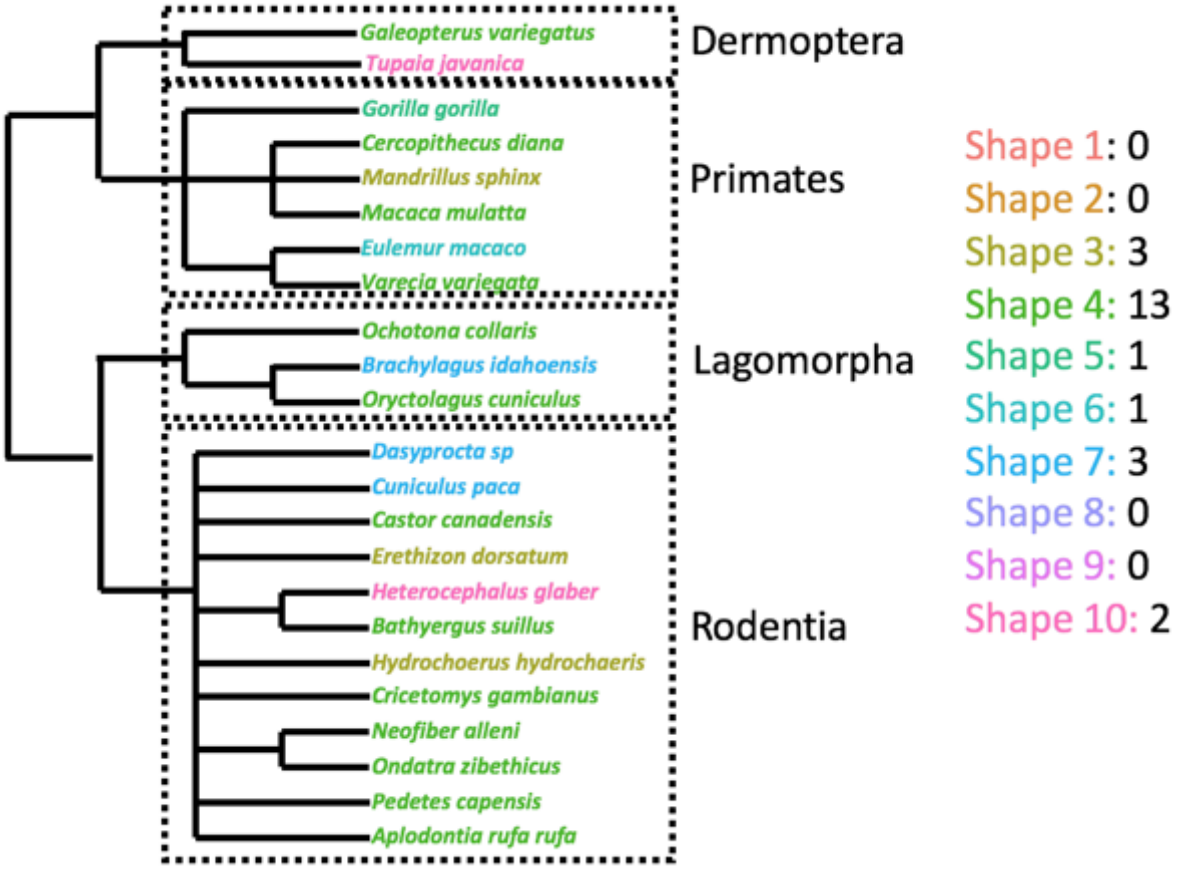

Figure 13. Representative phylogenetic tree of members of the superorder Euarchontoglires from this study with torso shape group identified by color.

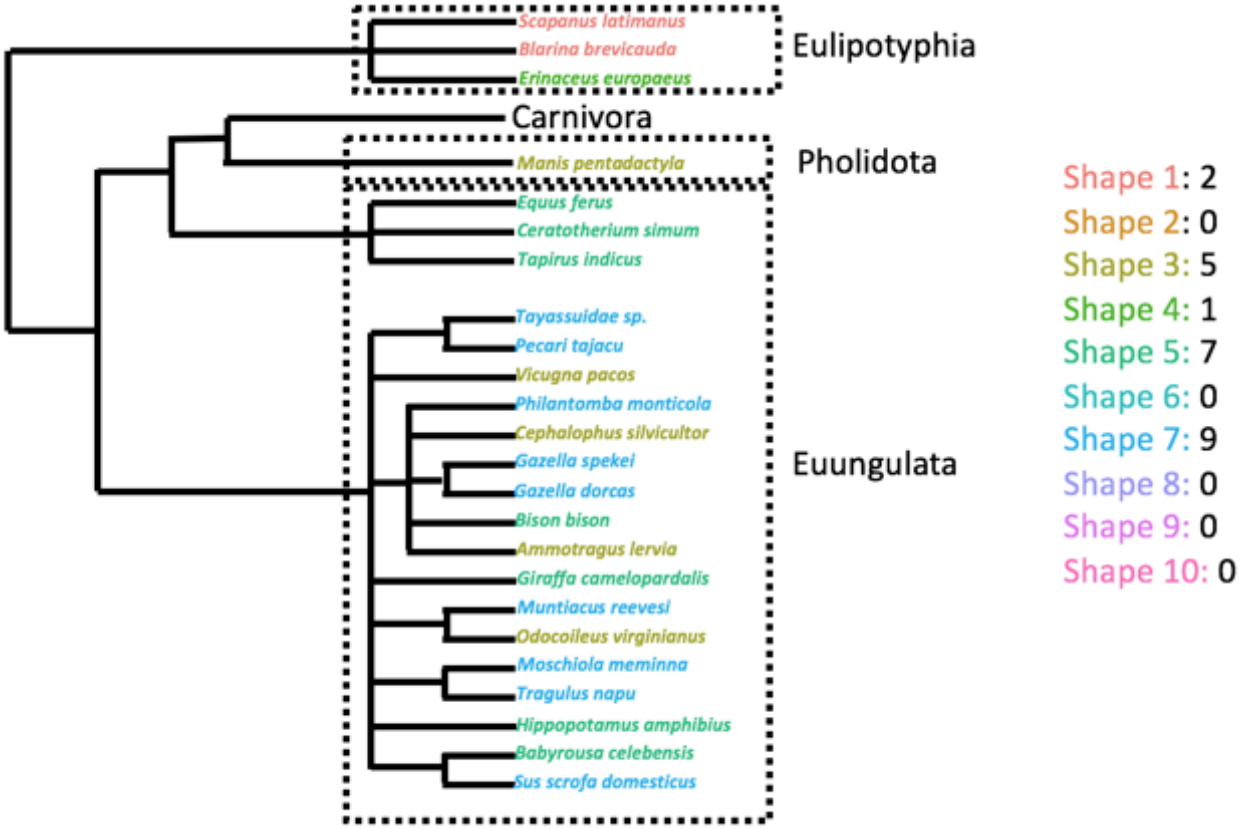

Figure 14. Representative phylogenetic tree of members of the superorder Laurasiatheria from this study with torso shape group identified by color

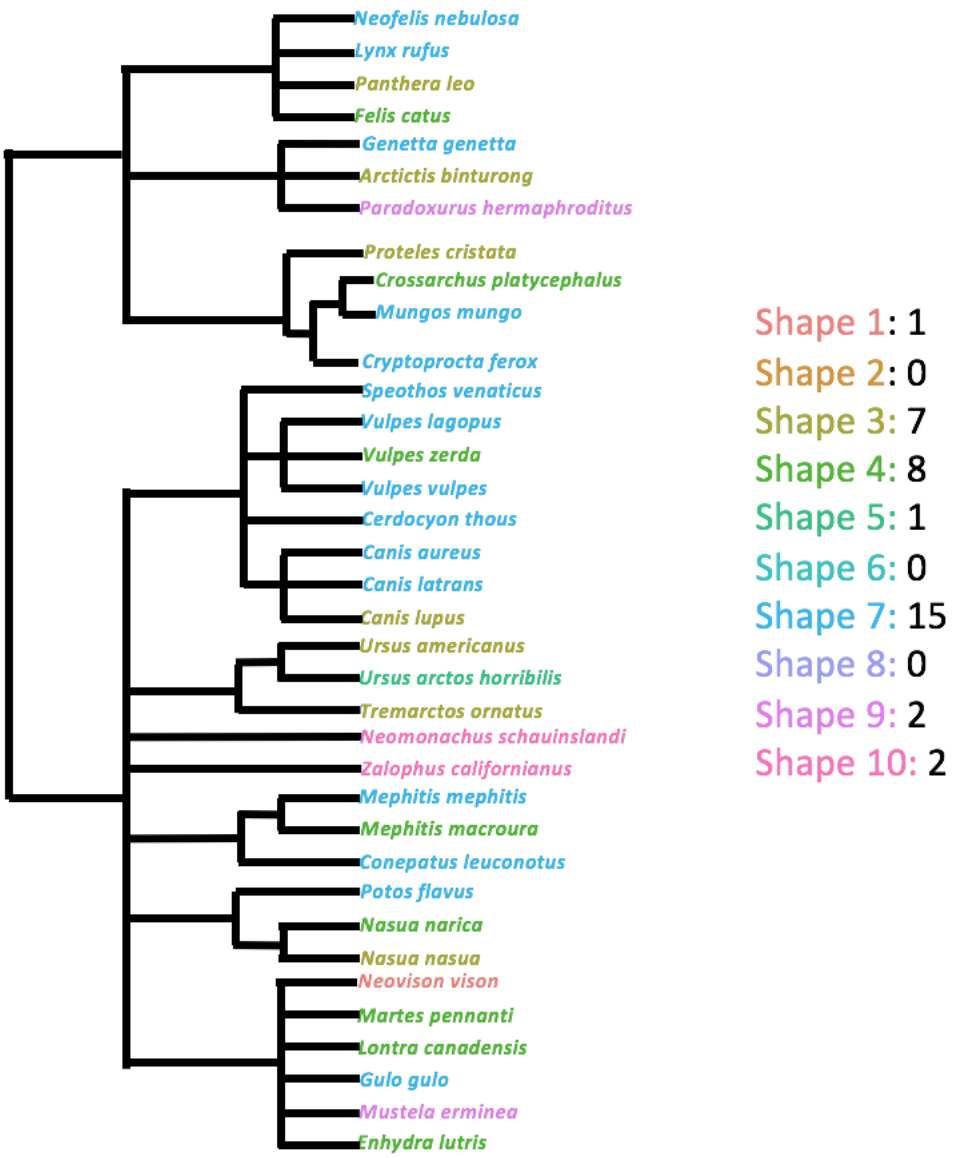

Figure 15. Representative phylogenetic tree of members of the Carnivora from this study with torso shape group identified by color

Appendix 1. Images of measured specimens with Species Code (see Table 2) in parentheses.

Reptiles

Alligator sinensis (1A)

Alligator sinensis (1B)

Alligator mississipiensis (2)

Caiman crocodilus yacare (3)

Caiman crocodilus (4)

Paleosuchus palpebrosus (5)

Crocodylus porosus (6)

Gavialis gangeticus (7)

Sphenodon punctatus (8)

Chondrodactylus bibronii (9)

Trachydosaurus rugosus (10)

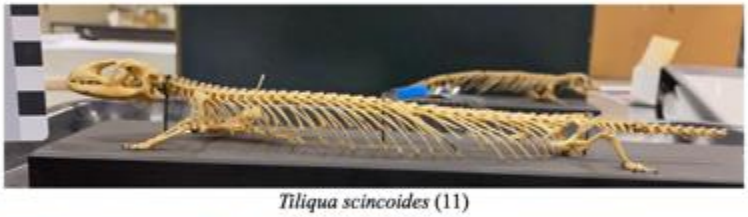

Tiliqua scincoides (11)

Salvator merianae (12)

Heloderma horridum (13)

Heloderma suspectum (14A)

Heloderma suspectum (14B)

Varanus griseus (15)

Varanus komodoensis (16)

Varanus macraei (17)

Varanus rudicollus (18)

Varanus salvator (19)

Bradypodion fischeri (20)

Uromastyx aegyptius (21)

Pogona vitticeps (22)

Dipsosaurus dorsalis (23)

Iguana iguana (24)

Mammals

Ornithorhynchus anatinus (25A)

Ornithorhynchus anatinus (25B)

Tachyglossus aculeatus (26)

Macropus parryi (27)

Petaurus breviceps (28)

Phascolarctos cinereus (29)

Sarcophilus harrisii (30)

Didelphis virginiana (31)

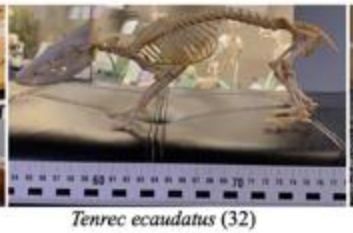

Tenrec ecaudatus (32)

Rhynchocyon petersi (33)

Orycteropus afer (34)

Loxodonta africana (35)

Procavia capensis (36)

Chaetophractus villosus (37)

Euphractus sexcinctus (38)

Dasypus novemcinctus (39)

Choloepus hoffmanni (40)

Myrmecophaga tridactyla (41)

Galeopterus variegatus (42)

Tupaia javanica (43)

Eulemur macaco (44)

Varecia variegata (45)

Cercopithecus diana (46)

Macaca mulatta (47)

Mandrillus sphinx (48)

Gorilla gorilla (49)

Brachylagus idahoensis (50)

Oryctolagus cuniculus (51)

Ochotona collaris (52)

Aplodontia rufa rufa (53)

Bathyergus suillus (54)

Castor canadensis (55)

Hydrochoerus hydrochaeris (56A)

Hydrochoerus hydrochaeris (56B)

Hydrochoerus hydrochaeris (56C)

Neofiber alleni alleni (57)

Ondatra zibethicus (58)

Cuniculus paca (59)

Dasyprocta *sp.* (60)

Heterocephalus glaber (61)

Erethizon dorsatum (62)

Cricetomys gambianus (63)

Pedetes capensis (64)

Erinaceus europaeus (65)

Scapanus latimanus (66)

Blarina brevicauda (67)

Canis aureus (68)

Canis latrans (69)

Canis lupus (70)

Cerdocyon thous (71)

Speothos venaticus (72)

Vulpes zerda (73)

Vulpes vulpes (74)

Vulpes lagopus lagopus (75)

Cryptoprocta ferox (76)

Felis catus (77)

Lynx rufus (78)

Neofelis nebulosa (79)

Panthera leo (80)

Conepatus leuconotus (81)

Mephitis macroura (82)

Mephitis mephitis (83)

Enhydra lutris (84)

Lontra canadensis (85A)

Lontra canadensis (85B)

Martes pennanti (86)

Mustela erminea (87)

Mustela vison (88)

Gulo gulo luscus (89)

Nasua narica narica (90)

Nasua nasua (91)

Potos flavus (92)

Crossarchus platycephalus (93)

Mungos mungo (94)

Proteles cristatus (95)

Zalophus californianus (96A)

Zalophus californianus (96B)

Monachus schauinslandi (97)

Tremarctos ornatus (98)

Ursus americanus (99)

Ursus arctos horribilis (100)

Arctictis binturong (101)

Genetta genetta (102)

Paradoxurus hermaphroditus (103)

Manis pentadactyla (104)

Equus ferus caballus (105)

Ceratotherium simum (106)

Tapirus indicus (107)

Ammotragus lervia (108)

Bison bison (109A)

Bison bison (109B)

Cephalophus silvicultor (110)

Gazella dorcas (111)

Gazella spekei (112)

Philantomba monticola (113)

Vicugna pacos (114)

Muntiacus reevesi (115)

Odocoileus virginianus (116)

Giraffa camelopardalis (117)

Hippopotamus amphibious (118)

Babyrousa celebensis (119)

Sus scrofa domesticus (120)

Pecari tajacu (121)

Tayassuidae *sp.* (122)

Moschiola memmina (123)

Tragulus napu borneanus (124)

Appendix 2. List of examined species and their species codes (SC), scientific name, common name, and taxonomic rank used throughout this study.

SC	Species	Common name	Order	Family
Reptilia				
1	*Alligator sinensis*	Chinese alligator	Crocodilia	Alligatoridae
2	*Alligator mississipiensis*	American alligator	Crocodilia	Alligatoridae
3	*Caiman crocodilus yacare*	Yacare caiman	Crocodilia	Alligatoridae
4	*Caiman crocodilus*	Spectacled caiman	Crocodilia	Alligatoridae
5	*Paleosuchus palpebrosus*	Cuvier's dwarf caiman	Crocodilia	Alligatoridae
6	*Crocodylus porosus*	Saltwater crocodile	Crocodilia	Crocodylidae
7	*Gavialis gangeticus*	Gharial	Crocodilia	Gavialidae
8	*Sphenodon punctatus*	Tuatara	Rhynchocephalia	Sphenodontidae
9	*Chondrodactylus bibronii*	Bibron's gecko	Squamata	Gekkonidae
10	*Trachydosaurus rugosus*	Shingleback lizard	Squamata	Scincidae
11	*Tiliqua scincoides*	Blue-tongued lizard	Squamata	Scincidae
12	*Salvator merianae*	Black and white tegu	Squamata	Teiidae
13	*Heloderma horridum*	Beaded lizard	Squamata	Helodermatidae
14	*Heloderma suspectum*	Gila monster	Squamata	Helodermatidae
15	*Varanus griseus*	Desert monitor	Squamata	Varanidae
16	*Varanus komodoensis*	Komodo dragon	Squamata	Varanidae
17	*Varanus macraei*	Blue tree monitor	Squamata	Varanidae
18	*Varanus rudicollis*	Rough-neck monitor	Squamata	Varanidae
19	*Varanus salvator*	Water monitor	Squamata	Varanidae
20	*Bradypodion fischeri*	Fischer's chameleon	Squamata	Chamaeleonidae
21	*Uromastyx aegypticus*	Egyptian mastigure	Squamata	Agamidae
22	*Pogona vitticeps*	Bearded dragon	Squamata	Agamidae
23	*Dipsosaurus dorsalis*	Desert iguana	Squamata	Iguanidae
24	*Iguana iguana*	Green iguana	Squamata	Iguanidae
Mammalia				
25	*Ornithorhynchus anatinus*	Platypus	Monotremata	Ornithorhynchidae
26	*Tachyglossus aculeatus*	Short-nosed echidna	Monotremata	Tachyglossidae
27	*Macropus parryi*	Pretty-faced wallaby	Diprotodontia	Macropodidae
28	*Petaurus breviceps*	Sugar glider	Diprotodontia	Petauridae
29	*Phascolarctos cinereus*	Koala	Diprotodontia	Phascolarctidae
30	*Sarcophilus harrisii*	Tasmanian devil	Dasyuromorphia	Dasyuridae
31	*Didelphis virginiana*	Virginia opossum	Didelphimorphia	Didelphidae
32	*Tenrec ecaudatus*	Common tenrec	Afrosoricida	Tenrecidae
33	*Rhynchocyon petersi*	Zanj elephant shrew	Macroscelidea	Macroscelididae
34	*Orycteropus afer*	Aardvark	Tubulidentata	Orycteropodidae
35	*Loxodonta africana*	African elephant	Proboscidea	Elephantidae
36	*Procavia capensis*	Rock hyrax	Hyracoidea	Procaviidae
37	*Chaetophractus villosus*	Big hairy armadillo	Cingulata	Chlamyphoridae

38	*Euphractus sexcinctus*	Six-banded armadillo	Cingulata	Chlamyphoridae
39	*Dasypus novemcinctus*	Nine-banded armadillo	Cingulata	Dasypodidae
40	*Choloepus hoffmanni*	Two-toed sloth	Pilosa	Choloepodidae
41	*Myrmecophaga tridactyla*	Giant anteater	Pilosa	Myrmecophagidae
42	*Galeopterus variegatus*	Malayan colugo	Dermoptera	Cynocephalidae
43	*Tupaia javanica*	Javan treeshrew	Scandentia	Tupaiidae
44	*Eulemur macaco*	Black lemur	Primates	Lemuridae
45	*Varecia variegata*	Black-and-white ruffed lemur	Primates	Lemuridae
46	*Cercopithecus diana*	Diana monkey	Primates	Cercopithecidae
47	*Macaca mulatta*	Rhesus macaque	Primates	Cercopithecidae
48	*Mandrillus sphinx*	Mandrill	Primates	Cercopithecidae
49	*Gorilla gorilla*	Western gorilla	Primates	Hominidae
50	*Brachylagus idahoensis*	Pygmy rabbit	Lagomorpha	Leporidae
51	*Oryctolagus cuniculus*	European rabbit	Lagomorpha	Leporidae
52	*Ochotona collaris*	Collared pika	Lagomorpha	Ochotonidae
53	*Aplodontia rufa rufa*	Mountain beaver	Rodentia	Aplodontiidae
54	*Bathyergus suillus*	Cape dune mole-rat	Rodentia	Bathyergidae
55	*Castor canadensis*	North American beaver	Rodentia	Castoridae
56	*Hydrochoerus hydrochaeris*	Capybara	Rodentia	Caviidae
57	*Neofiber alleni alleni*	Round-tailed muskrat	Rodentia	Cricetidae
58	*Ondatra zibethicus*	Muskrat	Rodentia	Cricetidae
59	*Cuniculus paca*	Lowland paca	Rodentia	Cuniculidae
60	*Dasyprocta sp.*	Agouti	Rodentia	Dasyproctidae
61	*Heterocephalus glaber*	Naked mole-rat	Rodentia	Heterocephalidae
62	*Erethizon dorsatum*	North American porcupine	Rodentia	Erethizontidae
63	*Cricetomys gambianus*	Gambian pouched rat	Rodentia	Nesomyidae
64	*Pedetes capensis*	Springhare	Rodentia	Pedetidae
65	*Erinaceus europaeus*	European hedgehog	Eulipotyphyla	Erinaceidae
66	*Scapanus latimanus*	Broad-footed mole	Eulipotyphyla	Talpidae
67	*Blarina brevicauda*	Northern short-tailed shrew	Eulipotyphyla	Soricidae
68	*Canis aureus*	Golden jackal	Carnivora	Canidae
69	*Canis latrans*	Coyote	Carnivora	Canidae
70	*Canis lupus*	Wolf	Carnivora	Canidae
71	*Cerdocyon thous*	Crab-eating fox	Carnivora	Canidae
72	*Speothos venaticus*	Bush dog	Carnivora	Canidae
73	*Vulpes zerda*	Fennec fox	Carnivora	Canidae
74	*Vulpes lagopus lagopus*	Arctic fox	Carnivora	Canidae
75	*Vulpes vulpes*	Red fox	Carnivora	Canidae
76	*Cryptoprocta ferox*	Fossa	Carnivora	Eupleridae
77	*Felis catus*	Domestic cat	Carnivora	Felidae
78	*Lynx rufus*	Bobcat	Carnivora	Felidae
79	*Neofelis nebulosa*	Clouded leopard	Carnivora	Felidae
80	*Panthera leo*	Lion	Carnivora	Felidae

81	*Conepatus leuconotus*	Hog-nosed skunk	Carnivora	Mephitidae
82	*Mephitis macroura*	Hooded skunk	Carnivora	Mephitidae
83	*Mephitis mephitis*	Striped skunk	Carnivora	Mephitidae
84	*Enhydra lutris*	Sea otter	Carnivora	Mustelidae
85	*Lontra canadensis*	Common otter	Carnivora	Mustelidae
86	*Martes pennanti*	Fisher	Carnivora	Mustelidae
87	*Mustela erminea*	Ermine	Carnivora	Mustelidae
88	*Mustela vison*	American mink	Carnivora	Mustelidae
89	*Gulo gulo luscus*	Wolverine	Carnivora	Mustelidae
90	*Nasua narica narica*	White-nosed coati	Carnivora	Procyonidae
91	*Nasua nasua*	South American coati	Carnivora	Procyonidae
92	*Potos flavus*	Kinkajou	Carnivora	Procyonidae
93	*Crossarchus platycephalus*	Flat-headed kusimanse	Carnivora	Herpestidae
94	*Mungos mungo*	Banded mongoose	Carnivora	Herpestidae
95	*Proteles cristatus*	Aardwolf	Carnivora	Hyaenidae
96	*Zalophus californianus*	California sea lion	Carnivora	Otariidae
97	*Monachus schauinslandi*	Hawaiian monk seal	Carnivora	Phocidae
98	*Tremarctos ornatus*	Spectacled bear	Carnivora	Ursidae
99	*Ursus americanus*	American black bear	Carnivora	Ursidae
100	*Ursus arctos horribilis*	Grizzly bear	Carnivora	Ursidae
101	*Arctictis binturong*	Binturong	Carnivora	Viverridae
102	*Genetta genetta*	Common genet	Carnivora	Viverridae
103	*Paradoxurus hermaphroditus*	Asian palm civet	Carnivora	Viverridae
104	*Manis pentadactyla*	Chinese pangolin	Pholidota	Manidae
105	*Equus ferus caballus*	Domestic horse	Perissodactyla	Equidae
106	*Ceratotherium simum*	White rhinoceros	Perissodactyla	Rhinocerotidae
107	*Tapirus indicus*	Malayan tapir	Perissodactyla	Tapiridae
108	*Ammotragus lervia*	Barbary sheep	Artiodactyla	Bovidae
109	*Bison bison*	American bison	Artiodactyla	Bovidae
110	*Cephalophus silvicultor*	Yellow-backed duiker	Artiodactyla	Bovidae
111	*Gazella dorcas*	Dorcas gazelle	Artiodactyla	Bovidae
112	*Gazella spekei*	Speke's gazelle	Artiodactyla	Bovidae
113	*Philantomba monticola*	Blue duiker	Artiodactyla	Bovidae
114	*Vicugna pacos*	Alpaca	Artiodactyla	Camelidae
115	*Muntiacus reevesi*	Reeve's muntjac	Artiodactyla	Cervidae
116	*Odocoileus virginianus*	White-tailed deer	Artiodactyla	Cervidae
117	*Giraffa camelopardalis*	Giraffe	Artiodactyla	Giraffidae
118	*Hippopotamus amphibious*	Hippopotamus	Artiodactyla	Hippopotamidae
119	*Babyrousa celebensis*	Sulawesi babirusa	Artiodactyla	Suidae
120	*Sus scrofa domesticus*	Domestic pig	Artiodactyla	Suidae
121	*Pecari tajacu*	Collared peccary	Artiodactyla	Tayassuidae
122	Tayassuidae *sp.*	Peccary	Artiodactyla	Tayassuidae
123	*Moschiola memmina*	Spotted mouse-deer	Artiodactyla	Tragulidae
124	*Tragulus napu borneanus*	Greater mouse-deer	Artiodactyla	Tragulidae

Appendix 3. Raw torso shape measurements taken from 132 amniote specimens examined (see Appendix 2).

SC	TTL	ATL	PTL	MTH	MTW	ATH	ATW	PTH	PTW	MHL	MFL
Reptilia											
1A	340	160	180	79	145	75	82	52	79	82	87
1B	270	94	176	67	95	40	55	60	61	77	87
2	322	150	172	51	116	29	52	39	78	85	90
3	530	310	220	120	234	76	153	105	160	136	171
4	390	149	241	54*	109	56	69	74	70	80	99
5	221	122	99	22*	82	20	42	50	58	54	70
6	435	175	260	110	210	105	130	76	115	110	126
7	545	270	275	64*	263	80	105	84	111	127	134
8**	140	74	66	34	56	27	36	19	33	32	40
9	49	25	24	11	8	8	10	8	12	9	13
10	109	70	39	19	46	14	15	16	16	14	15
11	165	84	81	23	50	16	21	19	27	24	21
12	225	125	100	80	120	36	46	39	54	60	61
13	300	160	140	58	106	32	41	30	43	53	59
14A	265	132	133	47	57	20	30	26	33	46	41
14B	219	121	98	30	87	10	17	14	20	24	30
15	210	74	136	37	80	29	35	28	28	44	49
16	585	400	185	189	310	145	164	150	155	126	160
17	146	71	75	8	33	5	7	11	12	25	24
18	160	83	77	18	69	19	26	28	27	37	40
19	490	223	267	109	190	63	108	74	85	91	116
20	84	33	51	22	3	10	6	13	4	19	20
21	139	84	55	24	66	20	28	16	33	29	31
22	135	95	40	37	72	20	27	29	32	36	42
23	82	39	43	12	30	9	11	19	19	22	29
24	229	126	103	52	109	39	44	56	48	66	78
Mammalia											
25A	125	50	75	58	69	26	35	35	28	40	33
25B	159	82	77	65	90	38	44	39	39	39	44
26	202	66	136	96	80	37	49	62	54	62	65
27	370	170	200	114	162	35	40	132	100	98	200
28	82	30	52	21	22	5	8	15	20	32	32
29	165	85	80	102	98	40	47	74	54	93	115
30	280	115	165	94	110	50	53	79	62	97	119
31	161	75	86	46	68	12	21	30	30	54	70
32	164	70	94	53	76	9	18	26	24	46	46
33	123	44	79	54	37	10	14	34	38	39	51
34	475	162	313	202	234	56	74	176	148	155	199
35	1870	760	1110	930	835	547	260	760	554	834	1050

36	255	119	136	86	80	39	35	59	64	70	73
37	186	80	106	70	100	19	28	42	54	62	70
38	231	105	126	99	162	42	72	72	73	84	96
39	200	70	130	109	124	32	43	48	87	165	90
40	350	159	191	118	131	34	63	119	107	148	146
41	434	222	212	216	199	65	78	165	130	160	216
42	229	92	137	76	80	12	24	42	39	109	128
43	76	34	42	23	22	8	9	7	22	29	31
44	242	71	171	77	61	31	27	4	39	87	119
45	281	144	137	77	91	18	48	65	62	104	143
46	355	163	192	109	98	24	41	82	73	138	170
47	300	120	180	109	80	20	41	65	58	130	150
48	520	190	330	174	112	62	68	112	120	233	310
49	755	312	443	222	422	142	163	245	252	410	355
50	145	60	85	44	36	20	14	21	31	49	59
51	184	82	102	81	55	16	20	44	44	66	84
52	85	44	41	35	34	5	13	24	11	29	31
53	146	52	94	50	53	11	23	30	28	37	47
54	132	66	66	53	64	11	15	26	38	43	51
55	315	130	185	110	200	25	42	49	95	85	110
56A	595	229	366	231	260	88	68	165	124	182	210
56B	520	222	298	215	199	55	49	153	101	160	184
56C	605	215	390	194	210	79	54	87	99	172	200
57	94	32	62	39	42	9	14	24	20	25	30
58	152	60	92	62	70	14	20	33	35	37	45
59	305	109	196	114	89	40	32	50	60	85	106
60	264	82	182	97	64	32	24	37	40	69	82
61	66	20	46	15	19	5	10	8	10	17	15
62	265	140	125	116	150	34	56	111	87	99	111
63	205	76	129	54	69	15	28	33	42	50	61
64	215	55	160	66	86	19	42	45	56	50	109
65	143	54	89	49	59	13	20	39	25	39	39
66	56	29	27	19	39	4	6	5	7	16	17
67	64	32	32	12	22	3	5	5	5	10	11
68	355	139	216	122	114	40	32	65	60	130	149
69	430	190	240	158	146	68	40	70	80	157	180
70	635	288	347	250	202	88	64	150	130	243	268
71	273	105	168	75	80	29	24	54	45	94	109
72	320	160	160	112	103	47	35	68	73	107	108
73	205	72	133	60	49	15	15	30	40	70	82
74	325	160	165	97	122	54	30	48	56	128	134
75	300	125	175	92	89	31	25	60	41	118	125
76	335	160	175	105	94	33	45	72	61	112	139
77	294	122	172	86	71	23	27	50	49	105	115
78	425	180	245	118	113	49	27	67	68	152	182
79	440	182	258	128	114	43	45	89	70	147	180

80	1020	430	590	345	320	155	115	235	145	345	410
81	184	95	89	78	69	22	13	55	45	69	82
82	151	64	87	55	47	17	19	44	34	50	59
83	168	73	95	67	50	22	14	36	39	60	73
84	620	250	370	185	260	40	60	60	86	112	139
85A	330	205	125	100	138	35	30	65	72	75	82
85B	364	131	233	94	101	21	40	35	46	80	79
86	264	129	135	70	69	16	23	51	40	80	96
87	130	59	71	27	24	10	8	12	14	30	34
88	183	69	114	45	47	9	6	10	12	40	39
89	494	226	268	128	153	58	52	80	65	143	145
90	209	85	124	69	75	19	24	59	45	83	104
91	263	130	133	100	99	42	44	64	63	99	124
92	214	72	142	73	62	26	30	48	60	68	85
93	173	68	105	55	62	20	19	42	28	53	59
94	205	80	125	66	53	28	20	40	48	59	77
95	312	132	180	100	121	28	44	72	73	140	142
96A	710	350	360	30	280	99	105	120	66	154	96
96B	900	414	486	269	253	102	115	49	64	162	84
97	1050	385	665	265	310	100	158	65	129	138	99
98	765	390	375	265	286	93	90	209	145	270	315
99	665	315	350	250	219	75	97	130	135	270	309
100	885	320	565	368	345	130	124	269	230	353	411
101	422	173	249	139	149	49	55	98	94	153	157
102	236	113	123	78	64	28	16	43	40	75	85
103	194	66	128	56	27	14	15	36	30	64	65
104	220	135	85	71	104	32	38	72	62	64	81
105	1140	545	595	520	528	226	119	324	294	335	410
106	1630	933	697	870	1109	360	140	515	410	355	500
107	1090	540	550	510	518	200	118	265	255	259	336
108	630	315	315	245	209	146	49	117	126	194	242
109A	1334	705	629	655	435	249	104	210	220	315	369
109B	1465	830	635	505*	520	295	176	296	264	340	438
110	695	281	414	254	242	134	64	132	132	194	239
111	450	235	215	159	176	62	33	99	85	111	140
112	470	240	230	190	160	85	39	80	90	125	169
113	312	132	180	107	102	41	21	50	49	85	110
114	680	325	355	275	265	125	54	160	120	200	280
115	424	152	272	235	109	68	33	64	65	114	138
116	740	310	430	280	305	140	79	133	125	190	255
117	1350	825	525	795	744	495	135	470	360	496	545
118	1600	817	783	810	806	402	169	402	401	384	515
119	635	320	315	315	272	134	65	190	142	230	231
120	930	359	571	259	265	122	56	98	125	195	210
121	470	185	285	175	162	75	34	92	76	154	170
122	419	154	265	139	123	62	28	59	74	145	147

123	294	116	178	89	88	49	25	23	54	82	96
124	226	104	122	75	57	30	20	36	37	80	92

* Maximum Rib Height (MRH) instead of MTH
** Measurements collected through palpation

Appendix 4. List of examined specimens. Abbreviations: SC, species code; Diet (C, carnivore; H, herbivore; I, insectivore); Sex (F, female; M, male); AC, age category (A, adult; SA, Subadult); LC, locality code (AF, Africa; AS, Asia; AU, Australia; CA, Central America; EU, Europe; NA, North America; NZ, New Zealand; SA, South America;); PC, preservation condition (SK, mounted complete skeleton; uSK, unmounted complete skeleton; pSK, partially disarticulated skeleton with articulated ribcage; PW, preserved whole animal)

SC	Species	Catalog number	Diet	Sex	AC	LC	PC
1A	*Alligator sinensis*	MoO 3754	C[14]	?	A	AS	SK
1B	*Alligator sinensis*	FMNH 31303	C[14]	F	SA	AS	pSK
2	*Alligator mississpiensis*	FMNH 31321	C[14]	F	SA	NA	pSK
3	*Caiman crocodilus yacare*	FMNH 9150	C[14]	?	?	SA	pSK
4	*Caiman crocodilus*	FMNH 13062	C[14]	?	?	SA	pSK
5	*Paleosuchus palpebrosus*	FMNH 98961	C[14]	?	?	?	pSK
6	*Crocodylus porosus*	MoO 3758	C[14]	?	A	?	SK
7	*Gavialis gangeticus*	MoO 3757	C[14]	?	A	AS	SK
8	*Sphenodon punctatus*	MNHC R0109	C[13]	?	?	NZ	PW
9	*Chondrodactylus bibronii*	FMNH 209448	C[12]	?	?	?	uSK
10	*Trachydosaurus rugosus*	FMNH 22035	H[6]	?	?	AU	SK
11	*Tiliqua scincoides*	FMNH 22034	H[6]	?	?	AU	SK
12	*Salvator merianae*	MoO 3523	O[8]	?	A	SA	SK
13	*Heloderma horridum*	MoO 3518	C[7]	?	A	CA	SK
14A	*Heloderma suspectum*	MoO 5443	C[7]	?	A	?	SK
14B	*Heloderma suspectum*	MNHC R0055	C[7]	?	?	NA	SK
15	*Varanus griseus*	FMNH 204663	C[4]	?	?	AF	SK
16	*Varanus komodoensis*	MoO 3524	C[4]	?	A	?	SK
17	*Varanus macraei*	MNHC R2099	C[9*]	?	?	?	uSK
18	*Varanus rudicollus*	MNHC R0091	C[4]	?	?	?	SK
19	*Varanus salvator*	MNHC R0089	C[4]	?	?	?	SK
20	*Bradypodion fischeri*	FMNH 229961	C[10]	?	?	?	pSK
21	*Uromastyx aegyptius*	FMNH 22031	H[6]	?	?	AF	SK
22	*Pogona vitticeps*	MoO 6348	O[11]	?	A	AU	SK
23	*Dipsosaurus dorsalis*	FMNH 206188	H[6]	?	?	?	pSK
24	*Iguana iguana*	MoO 3529	H[5]	?	A	SA	SK
25A	*Ornithorhynchus anatinus*	FMNH 81527	C[3]	?	A	AU	SK
25B	*Ornithorhynchus anatinus*	MoO 3813	C[3]	?	A	AU	SK
26	*Tachyglossus aculeatus*	MoO 3817	C[3]	?	A	AU	SK
27	*Macropus parryi*	MoO 3780	H[1]	?	A	AU	SK
28	*Petaurus breviceps*	MoO 3785	O[1]	?	A	AU	SK
29	*Phascolarctos cinereus*	MoO 1624	H[3]	?	A	AU	SK
30	*Sarcophilus harrisii*	MoO 3775	C[3]	?	A	AU	SK
31	*Didelphis virginiana*	MNHC TC460	O[1]	?	?	NA	SK
32	*Tenrec ecaudatus*	MoO 3792	C[3]	?	A	AF	SK
33	*Rhynchocyon petersi*	MoO 3811	C[1]	?	A	AF	SK
34	*Orycteropus afer*	MoO 3886	C[3]	?	A	?	SK

35	*Loxodonta africana*	MoO 4710	H^2	?	A	AF	SK
36	*Procavia capensis*	MoO 3873	H^3	?	A	AF	SK
37	*Chaetophractus villosus*	MNHC 33	O^3	?	?	SA	SK
38	*Euphractus sexcinctus*	MoO 3841	O^3	?	A	SA	SK
39	*Dasypus novemcinctus*	MoO 3501	C^2	?	A	NA	SK
40	*Choloepus hoffmanni*	MoO 2163	H^3	?	A	C/SA	SK
41	*Myrmecophaga tridactyla*	MoO 3850	C^1	?	A	?	SK
42	*Galeopterus variegatus*	MoO 1098	H^3	?	A	AS	SK
43	*Tupaia javanica*	MoO 3827	C^3	?	A	AS	SK
44	*Eulemur macaco*	MNHC 41	H^1	?	?	AF	SK
45	*Varecia variegata*	MoO 2781	H^3	?	A	AF	SK
46	*Cercopithecus diana*	MoO 2723	O^1	?	A	AF	SK
47	*Macaca mulatta*	FMNH 59018	H^3	F	A	?	SK
48	*Mandrillus sphinx*	MoO 08-579/784	H^2	M	A	AF	SK
49	*Gorilla gorilla*	MoO 2793	H^3	?	A	AF	SK
50	*Brachylagus idahoensis*	MoO 3806	H^3	?	A	NA	SK
51	*Oryctolagus cuniculus*	MoO 6328	H^3	?	A	?	SK
52	*Ochotona collaris*	MoO 3273	H^3	?	A	NA	SK
53	*Aplodontia rufa rufa*	FMNH 18820	H^3	M	A	NA	SK
54	*Bathyergus suillus*	MoO 2159	H^1	?	A	AF	SK
55	*Castor canadensis*	MoO 3489	H^1	?	A	NA	SK
56A	*Hydrochoerus hydrochaeris*	MoO 3860	H^3	?	A	SA	SK
56B	*Hydrochoerus hydrochaeris*	FMNH 51636	H^3	?	A	SA	SK
56C	*Hydrochoerus hydrochaeris*	MNHC 6029	H^3	?	?	SA	SK
57	*Neofiber alleni alleni*	FMNH 18824	H^3	F	A	NA	SK
58	*Ondatra zibethicus*	MoO 3488	H^3	?	A	NA	SK
59	*Cuniculus paca*	FMNH 15613	H^3	?	A	SA	SK
60	Dasyprocta sp.	MNHC 17	H^{1*}	?	?	SA	SK
61	*Heterocephalus glaber*	FMNH 1439	H^1	F	A	AF	SK
62	*Erethizon dorsatum*	MoO 3859	H^3	?	A	NA	SK
63	*Cricetomys gambianus*	MoO 3855	O^1	?	A	AF	SK
64	*Pedetes capensis*	MNHC 6027	H^3	?	?	?	SK
65	*Erinaceus europaeus*	MoO 6123	C^1	?	A	?	SK
66	*Scapanus latimanus*	MoO 3830	C^2	?	A	NA	SK
67	*Blarina brevicauda*	MoO 3504	C^2	?	A	?	SK
68	*Canis aureus*	FMNH 15536	C^3	?	A	AS	SK
69	*Canis latrans*	MoO 3436	C^3	F?	A	NA	SK
70	*Canis lupus*	MoO 3437	C^3	M	A	?	SK
71	*Cerdocyon thous*	FMNH 15538	C^3	?	A	SA	SK
72	*Speothos venaticus*	MoO 3455	C^3	F?	A	SA	SK
73	*Vulpes zerda*	MoO 3456	C^3	?	A	AF	SK
74	*Vulpes vulpes*	MoO 3500	C^2	?	A	?	SK
75	*Vulpes lagopus lagopus*	FMNH 15537	C^2	?	A	EU	SK
76	*Cryptoprocta ferox*	MoO 3396	C^3	M	A	AF	SK
77	*Felis catus*	MoO 2724	C^3	?	A	?	SK
78	*Lynx rufus*	MoO 3498	C^3	?	A	NA	SK

79	*Neofelis nebulosa*	MoO 5442	C^3	?	A	AS	SK
80	*Panthera leo*	MoO 3431	C^3	?	A	AF	SK
81	*Conepatus leuconotus*	MoO 14320/3393	C^3	M	A	N/CA	SK
82	*Mephitis macroura*	MoO 3404	O^3	F?	A	N/CA	SK
83	*Mephitis mephitis*	MoO 3497	O^3	?	A	?	SK
84	*Enhydra lutris*	MoO 3397	C^3	M	A	NA	SK
85A	*Lontra canadensis*	MoO 3496	C^3	?	A	NA	SK
85B	*Lontra canadensis*	MNHC 56	C^3	M	?	NA	SK
86	*Martes pennanti*	FMNH 15539	C^3	?	A	NA	SK
87	*Mustela erminea*	MNHC 63	C^3	M	?	NA	SK
88	*Mustela vison*	MNHC 58	C^3	M	?	NA	SK
89	*Gulo gulo luscus*	FMNH 15541	C^3	?	A	NA	SK
90	*Nasua narica narica*	FMNH 15543	O^3	?	A	NA	SK
91	*Nasua nasua*	MoO 3424	O^3	M	A	?	SK
92	*Potos flavus*	MoO 3411	H^3	F?	A	C/SA	SK
93	*Crossarchus platycephalus*	MoO 3395	C^1	F?	A	AF	SK
94	*Mungos mungo*	MoO 3406	C^3	F?	A	AF	SK
95	*Proteles cristatus*	MoO 3412	C^3	F?	A	AF	SK
96A	*Zalophus californianus*	MoO 3479	C^3	?	A	NA	SK
96B	*Zalophus californianus*	MNHC 22	C^3	?	?	NA	SK
97	*Monachus schauinslandi*	MoO 3468	C^3	?	A	?	SK
98	*Tremarctos ornatus*	MoO 3417	H^3	M	A	SA	SK
99	*Ursus americanus*	FMNH 15547	H^3	?	A	NA	uSK
100	*Ursus arctos horribilis*	MoO 6907	O^{15}	M	A	NA	SK
101	*Arctictis binturong*	MoO 3392	O^3	F?	A	AS	SK
102	*Genetta genetta*	MoO 3398	C^3	F?	A	AF	SK
103	*Paradoxurus hermaphroditus*	FMNH 15534	O^3	?	A	AS	SK
104	*Manis pentadactyla*	MoO 3822	C^3	?	A	AS	SK
105	*Equus ferus caballus*	MoO 3995	H^3	?	A	?	SK
106	*Ceratotherium simum*	MoO 4707	H^3	F	A	AF	SK
107	*Tapirus indicus*	MoO 3987	H^1	?	A	?	SK
108	*Ammotragus lervia*	MoO 3940	H^2	?	A	NA?	SK
109A	*Bison bison*	FMNH 15577	H^3	?	A	NA	SK
109B	*Bison bison*	MoO 3494	H^3	?	A	NA	SK
110	*Cephalophus silvicultor*	MoO 3915	H^2	?	A	AF	SK
111	*Gazella dorcas*	MoO 3927	H^1	?	A	AF	SK
112	*Gazella spekei*	FMNH 18809	H^1	?	A	AF	SK
113	*Philantomba monticola*	MoO 3933	H^1	?	A	AF	SK
114	*Vicugna pacos*	MoO 3973	H^{16}	?	A	SA	SK
115	*Muntiacus reevesi*	MoO 3954	H^1	M	A	AS	SK
116	*Odocoileus virginianus*	MoO 3492	H^3	?	A	?	SK
117	*Giraffa camelopardalis*	MoO 4708	H^3	M	A	AF	SK
118	*Hippopotamus amphibious*	MoO 4709	H^3	M	A	AF	SK
119	*Babyrousa celebensis*	MoO 3971	H^3	?	A	AS	SK
120	*Sus scrofa domesticus*	MNHC 6028	H^3	?	?	?	SK
121	*Pecari tajacu*	MoO 3972	H^3	?	A	?	SK

122	Tayassuidae *sp.*	MNHC 31	H[2**]	?	?	?	SK
123	*Moschiola memmina*	MoO 3952	H[3]	?	A	AS	SK
124	*Tragulus napu borneanus*	FMNH 15570	H[3]	?	A	SA	SK

* Indicates extrapolated from related taxa – genus

** Indicates extrapolated from related taxa – family

[1]Diet data from MammalDiet and MammalDiet2 metadata (Kissling et al., 2014; Gainsbury et al., 2017)

[2]Diet data from Pineda-Munoz and Alroy (2014)

[3]Diet data from PHYLACINE 1.2 (Faurby et al., 2018)

[4]Diet data from Losos & Greene, 1988

[5]Diet data from Troyer, 1984

[6]Diet data from Pough, 1973

[7]Diet data from Beck, 1990

[8]Diet data from Engemen et al., 2019

[9]Diet data from Ziegler et al., 2009

[10]Diet data from da Silva et al., 2016

[11]Diet data from Oonincx et al., 2015

[12]Diet data from Pianka and Huey, 1978

[13]Diet data from Cartland-Shaw et al., 1998

[14]Diet data from Erickson et al., 2012

[15]Diet data from Hilderbrand et al., 1996

[16]Diet data from St-Pierre and Wright, 2012

Appendix 5. Raw coordinate data for principal component analysis (PCA) on Torso Shape Groups.

Scientific Name	Common Name	PC1	PC2
Alligator sinensis	Chinese alligator	-0.5541519	-0.3254875
Alligator mississpiensis	American alligator	0.10344772	-0.0187798
Caiman crocodilus yacare	Yacare caiman	0.06675091	-0.0216572
Caiman crocodilus	Spectacled caiman	0.13423394	0.00724906
Paleosuchus palpebrosus	Cuvier's dwarf caiman	0.08814877	-0.0496756
Crocodylus porosus	Saltwater crocodile	0.116786	-0.0424415
Gavialis gangeticus	Gharial	0.20268522	0.02074641
Sphenodon punctatus	Tuatara	0.15789085	-0.0163861
Chondrodactylus bibronii	Bibron's gecko	0.12951259	-0.0018778
Trachydosaurus rugosus	Shingleback lizard	0.14251224	-0.059749
Tiliqua scincoides	Blue-tongued lizard	0.14219482	-0.0449145
Salvator merianae	Black and white tegu	0.15074415	-0.0615228
Heloderma horridum	Beaded lizard	0.15410928	-0.0207718
Heloderma suspectum	Gila monster	0.15383668	-0.0240801
Varanus griseus	Desert monitor	0.13186051	0.00505355
Varanus komodoensis	Komodo dragon	0.2016425	-0.0228454
Varanus macraei	Blue tree monitor	0.18153556	0.01892307
Varanus rudicollus	Rough-neck monitor	0.1338355	-0.0527551
Varanus salvator	Water monitor	0.15772758	-0.0338748
Bradypodion fischeri	Fischer's chameleon	0.04676116	0.00831712
Uromastyx aegyptius	Egyptian mastigure	0.12198335	0.0386974
Pogona vitticeps	Bearded dragon	0.10680618	-0.0013743
Dipsosaurus dorsalis	Desert iguana	0.09226186	-0.0126483
Iguana iguana	Green iguana	-0.1127098	-0.0198725
Ornithorhynchus anatinus	Platypus	-0.0043317	0.04060111
Tachyglossus aculeatus	Short-nosed echidna	-0.0194286	-0.0359357
Macropus parryi	Pretty-faced wallaby	-0.0366347	-0.0785847
Petaurus breviceps	Sugar glider	-0.2089431	-0.0292013
Phascolarctos cinereus	Koala	-0.0990686	-0.0026464
Sarcophilus harrisii	Tasmanian devil	-0.0681217	-8.70E-05
Didelphis virginiana	Virginia opossum	0.0498755	0.06308703
Tenrec ecaudatus	Common tenrec	-0.1005681	-0.0378215
Rhynchocyon petersi	Zanj elephant shrew	-0.038227	-0.0168059
Orycteropus afer	Aardvark	0.01036806	0.02971745
Loxodonta africana	African elephant	-0.1696894	0.01837016
Procavia capensis	Rock hyrax	-0.0741746	-0.0993856
Chaetophractus villosus	Big hairy armadillo	-0.0643036	-0.0242763

Euphractus sexcinctus	Six-banded armadillo	-0.1654068	-0.071462
Dasypus novemcinctus	Nine-banded armadillo	-0.0818569	-0.0473586
Choloepus hoffmanni	Two-toed sloth	-0.0228191	0.03482402
Myrmecophaga tridactyla	Giant anteater	-0.0430308	0.01376991
Galeopterus variegatus	Malayan colugo	-0.1204316	-0.0335716
Tupaia javanica	Javan treeshrew	-0.0571538	-0.0461665
Eulemur macaco	Black lemur	-0.1073719	0.03451231
Varecia variegata	Black-and-white ruffed lemur	0.03889929	0.02628471
Cercopithecus diana	Diana monkey	-0.0035634	-0.0249386
Macaca mulatta	Rhesus macaque	-0.0941595	0.0276287
Mandrillus sphinx	Mandrill	-0.0268543	-0.0650253
Gorilla gorilla	Western gorilla	-0.0113575	-0.0408409
Brachylagus idahoensis	Pygmy rabbit	0.26916291	-0.0043629
Oryctolagus cuniculus	European rabbit	0.36514122	-0.0452263
Ochotona collaris	Collared pika	0.28026127	0.05714957
Aplodontia rufa rufa	Mountain beaver	0.26208156	-0.036439
Bathyergus suillus	Cape dune mole-rat	0.31275865	-0.0313153
Castor canadensis	North American beaver	0.24202156	-0.0259774
Hydrochoerus hydrochaeris	Capybara	0.20519161	-0.0271283
Neofiber alleni alleni	Round-tailed muskrat	0.35107516	-0.0507351
Ondatra zibethicus	Muskrat	0.30099879	-0.0292592
Cuniculus paca	Lowland paca	0.21776302	-0.0621215
Dasyprocta sp.	Agouti	0.27496601	0.10010696
Heterocephalus glaber	Naked mole-rat	0.23227291	-0.0193447
Erethizon dorsatum	North American porcupine	0.23030342	0.07984834
Cricetomys gambianus	Gambian pouched rat	0.22732303	-0.0322187
Pedetes capensis	Springhare	-0.1882493	0.12680798
Erinaceus europaeus	European hedgehog	-0.1966771	0.11226796
Scapanus latimanus	Broad-footed mole	-0.0783862	0.19296843
Blarina brevicauda	Northern short-tailed shrew	-0.206816	0.08926347
Canis aureus	Golden jackal	-0.031597	0.12744292
Canis latrans	Coyote	-0.0383647	0.17387336
Canis lupus	Wolf	-0.0775779	0.09906427
Cerdocyon thous	Crab-eating fox	-0.2418215	0.08947419
Speothos venaticus	Bush dog	-0.0812447	0.09176681
Vulpes zerda	Fennec fox	-0.114685	0.16517904
Vulpes lagopus lagopus	Arctic fox	-0.3955224	0.0401552
Vulpes vulpes	Red fox	-0.3022749	0.01590042
Cryptoprocta ferox	Fossa	-0.2812928	0.02531252
Felis catus	Domestic cat	-0.3866951	-0.0525497

Lynx rufus	Bobcat	-0.3088931	-0.0395009
Neofelis nebulosa	Clouded leopard	-0.2020375	-0.1348189
Panthera leo	Lion	-0.5766894	0.12519339
Conepatus leuconotus	Hog-nosed skunk	-0.4263802	0.10006053
Mephitis macroura	Hooded skunk	-0.6290288	0.06803292
Mephitis mephitis	Striped skunk	-0.4603401	-0.0739378
Enhydra lutris	Sea otter	0.08086804	0.08852475
Lontra canadensis	Common otter	0.10624985	0.08061185
Martes pennanti	Fisher	0.18526264	0.1342526
Mustela erminea	Ermine	0.03141243	0.0793469
Mustela vison	American mink	0.20112215	0.11322431
Gulo gulo luscus	Wolverine	0.09064012	0.16521637
Nasua narica narica	White-nosed coati	-0.0027023	0.13461982
Nasua nasua	South American coati	0.08628493	0.09837472
Potos flavus	Kinkajou	0.13969538	0.05203671
Crossarchus platycephalus	Flat-headed kusimanse	0.01936197	0.07210263
Mungos mungo	Banded mongoose	0.02756629	0.06946478
Proteles cristatus	Aardwolf	0.091035	0.08191346
Zalophus californianus	California sea lion	0.01688338	0.12249931
Monachus schauinslandi	Hawaiian monk seal	-0.2488377	0.07904137
Tremarctos ornatus	Spectacled bear	-0.1281016	-0.0527877
Ursus americanus	American black bear	0.00942687	-0.0540963
Ursus arctos horribilis	Grizzly bear	-0.0720299	-0.0836789
Arctictis binturong	Binturong	0.02055077	-0.0387003
Genetta genetta	Common genet	0.074412	-0.0488747
Paradoxurus hermaphroditus	Asian palm civet	0.09111094	-0.0524171
Manis pentadactyla	Chinese pangolin	-0.0309199	-0.0699526
Equus ferus caballus	Domestic horse	0.039742	-0.1234279
Ceratotherium simum	White rhinoceros	0.03251952	-0.0363405
Tapirus indicus	Malayan tapir	0.06471736	-0.076033
Ammotragus lervia	Barbary sheep	0.00542601	-0.0688949
Bison bison	American bison	-0.0621137	-0.0074391
Cephalophus silvicultor	Yellow-backed duiker	-0.069905	-0.0649958
Gazella dorcas	Dorcas gazelle	0.00541029	-0.0510656
Gazella spekei	Speke's gazelle	0.06502797	-0.0388734
Philantomba monticola	Blue duiker	-0.050102	-0.0476534
Vicugna pacos	Alpaca	0.06571661	-0.0327737
Muntiacus reevesi	Reeve's muntjac	-0.0471502	-0.0605424
Odocoileus virginianus	White-tailed deer	0.01785957	-0.0056852
Giraffa camelopardalis	Giraffe	0.02070888	-0.0148959

Hippopotamus amphibious	Hippopotamus	-0.0277731	-0.0614275
Babyrousa celebensis	Sulawesi babirusa	0.01214292	-0.0395792
Sus scrofa domesticus	Domestic pig	-0.0022085	-0.1065408
Pecari tajacu	Collared peccary	0.01817654	-0.0002587
Tayassuidae sp.	Peccary	-0.0334774	-0.067649
Moschiola memmina	Spotted mouse-deer	-0.0744121	-0.0857174
Tragulus napu borneanus	Greater mouse-deer	-0.0483965	-0.0988208

Appendix 6. Loadings for principal components by Torso Shape Variable.

	PC1	PC2
ATL	0.10809565	0.1427448
PTL	0.03894177	-0.1870125
MTH	0.32357137	-0.576968
MTW	0.30819915	0.47209971
ATH	0.51548882	-0.0916769
ATW	0.38378595	0.51049177
PTH	0.46363443	-0.3324819
PTW	0.39891912	0.09658843